that in each sample from the KS661-infected monkeys. However, unlike the KS661 proviral DNA levels, the #64 proviral DNA levels in most tissues were maintained up to 27 dpi. These results suggest that #64 spread more slowly than KS661 and that the amounts of proviral DNA in a variety of tissues from the #64-infected animals were smaller than those in the tissues from KS661-infected animals around the initial peak of plasma viremia.

Because the amount of proviral DNA measured by PCR may include nonreplicating remnants of the viral genome, we also measured the number of IVPCs in each tissue sample by a plaque assay as described previously (9, 15). Briefly, cells prepared from infected animals were mixed with human T-lymphoid M8166 indicator cells, resuspended in culture medium containing 0.4% agarose, and plated into petri dishes. The plaques that formed in the cell layer were counted after 10 days of cultivation, and the number of IVPCs was calculated. For the KS661-infected monkeys, high numbers of IVPCs in all the tissue samples examined at 13 dpi were detected (Fig. 2B). Among these samples, the thymus and mesenteric LN samples harbored especially high numbers of IVPCs (more than 500/10^6 cells) at 13 dpi. The numbers of IVPCs declined remarkably from 13 to 27 dpi. We concluded that KS661 replicated systemically and synchronously in a variety of tissues, including the intestinal tract, at 13 dpi. In contrast, #64 production patterns in different tissues were not synchronous. Among #64-infected monkeys at 6 dpi, virus production was most active in the jejunum lamina propria lymphocytes (LPL) of MM390 (166 IVPCs/10^6 cells). At 13 dpi, interestingly, mesenteric LN became the center of virus production in two of the three monkeys examined (MM372 and MM373; 259 and 160 IVPCs/10^6 cells). In the other monkey (MM391), the jejunum had the highest number of IVPCs, followed by the mesenteric LN. These results suggested that the virus that replicated in the jejunum spread directly into the mesenteric LN via the flow of lymphatic fluid. At 27 dpi, the thymus tissues of both monkeys examined (MM374 and MM378) exhibited the highest numbers of IVPCs. In summary, the systemic dissemination of #64 was slower than that of KS661, and it was particularly delayed in the thymus during the acute phase.

Systemic $CD4^+$ cell depletion is the signature of disease induced by highly pathogenic SHIVs (7, 8, 22). We therefore compared the frequencies of $CD4^+$ cells in tissues from the animals infected with KS661 and #64, in addition to those of the circulating $CD4^+$ T lymphocytes. As representatives of the major virus-producing organs, the thymus, the mesenteric LN, and the jejunum were selected for examination. CD4 cell numbers were measured by immunohistochemistry analyses as described previously (18). Uninfected thymus tissue contained abundant $CD4^+$ cells that were stained brown (Fig. 3A, panel a), while the tissue collected from the KS661-infected animal at 27 dpi harbored few such cells (Fig. 3A, panel b). #64 caused virtually no $CD4^+$ cell depletion in the thymus at 27 dpi (Fig. 3A, panel c). In the mesenteric LN of uninfected monkeys, $CD4^+$ cells were found in the paracortical region (Fig. 3A, panel d). KS661 depleted $CD4^+$ cells in this area (Fig. 3A, panel e). Unlike KS661, #64 did not reduce the level of $CD4^+$ cells (Fig. 3A, panel f). The jejunum samples from uninfected animals contained $CD4^+$ cells in the lamina propria and follicles of gut-associated lymphatic tissues (Fig. 3 A, panel g). KS661 depleted $CD4^+$ cells in these tissues, too (Fig. 3A, panel h). Interestingly, #64 caused $CD4^+$ cell depletion in the small intestine comparable to that caused by KS661 (Fig. 3A, panel i). To confirm the observed cell reduction in the jejunum samples, we randomly selected a total of 40 fields on the tissue sections from each animal for viewing at a total magnification of ×400, counted $CD4^+$ cells, and averaged the numbers (Fig. 3B). The $CD4^+$ cell densities in the jejunum samples from the #64-infected monkeys were significantly lower than those in the samples from uninfected animals ($P < 0.001$). This gut-specific $CD4^+$ cell depletion caused by #64 prompted us to analyze the frequencies of $CD4^+$ T cells (including CD4 and CD8 doubly positive cells) in a variety of tissues by flow cytometry (Fig. 3C). KS661 caused systemic $CD4^+$ T-lymphocyte depletion by 27 dpi (Fig. 3C). In agreement with the immunohistochemistry results, #64 significantly depleted $CD4^+$ T cells only in the jejunum intraepithelial lymphocytes and LPL ($P = 0.01$ and 0.003, respectively) (Fig. 3C) by 27 dpi, although we examined only two #64-infected monkeys at 27 dpi. In conclusion, the $CD4^+$ T-cell depletion patterns caused by KS661 and #64 were distinct, and the small intestine was the only site in which $CD4^+$ T cells were significantly depleted by the moderately pathogenic #64.

Taken together, our results show that #64 disseminated more slowly and replicated less than KS661 in systemic lymphoid tissues, as well as in peripheral blood, during the acute phase of infection. We believe that because of its low rate and low levels of replication, #64 could not cause irreversible injury before the host mounted an immune reaction. As a result, $CD4^+$ T cells were not completely depleted in all the tissues examined, except in the small intestine. These results suggest that the small intestine is the tissue most sensitive to virus-induced $CD4^+$ T-cell depletion during the acute phase of infection. Recent reports revealed that severe acute depletions

FIG. 3. Profiles of $CD4^+$ T cells in systemic lymphoid tissues during acute infection. (A) Immunohistochemical staining for CD4 molecules (stained brown) in the thymus, mesenteric (mes.) LN, and jejunum tissues of KS661- or #64-infected monkeys at 27 dpi, in addition to those of uninfected monkeys. Black scale bars, 100 μm; white scale bars in insets of panels g, h, and i, 50 μm. (B) Comparison of $CD4^+$ cell frequencies in the jejunum LPL of uninfected and #64-infected monkeys at 27 dpi. A total of forty randomly selected fields (total magnification, ×400) of at least four tissue sections per animal were used for the analysis of jejunum LPL. *P* values (determined by Student's *t* test with 95% confidence intervals) are for comparisons of each #64-infected monkey with uninfected monkeys. (C) Percentages of $CD4^+$ T cells among total lymphocytes from KS661- and #64-infected monkeys. In each graph, data for 0 dpi (time points postinfection are shown along the *x* axis) are averages of percentages for seven uninfected control monkeys. Percentages of $CD4^+$ T cells (including CD4 and CD8 doubly positive cells) were obtained by first gating lymphocytes and then $CD3^+$ T cells with a flow cytometer. PBMC, peripheral blood mononuclear cells; Ing., inguinal; Jej., jejunum; iEL, intraepithelial lymphocytes; BM, bone marrow; Col., colon; *, $P < 0.05$ (percentage at 0 dpi versus that at 27 dpi; Student's *t* test with a 95% confidence interval).

of mucosal $CD4^+$ T cells have been observed in simian immunodeficiency virus-infected monkeys (11, 12, 24, 25) and human immunodeficiency virus-infected humans (2, 5, 13). The acute depletion of mucosal $CD4^+$ T cells and the disease outcome are correlated (1, 3, 21, 26). However, a decrease of mucosal $CD4^+$ T cells has also been observed in the early phases of natural host infections, such as SIVagm infection in African green monkeys and SIVsmm infection in sooty mangabeys, which typically do not progress to AIDS (4, 14, 19). In addition, the levels of apoptosis and immune activation and the degrees of $CD4^+$ T-cell restoration differ between progressors and nonprogressors in simian immunodeficiency virus models (4, 14, 19). Taken together, these results raise the possibility that the severe acute depletion of mucosal $CD4^+$ T cells is not sufficient to induce AIDS. The restoration of $CD4^+$ T cells and normal immune function after the severe acute depletion may define the eventual disease outcome (20). The abilities of KS661- and #64-infected monkeys to restore the immune system may be different, because KS661, but not #64, impairs thymic T-cell differentiation (18). Currently, we are focusing on the restoration of $CD4^+$ T cells and the functional aspect of the immune cells in the small intestines of animals infected with KS661 and #64 to further clarify the determinant(s) of the disease outcome.

We are grateful to James Raymond for English editing of the manuscript and to Takahito Kazama for technical support.

This work was supported, in part, by Research on Human Immunodeficiency Virus/AIDS in Health and Labor Sciences research grants from the Ministry of Health, Labor and Welfare, Japan, a grant-in-aid for scientific research from the Ministry of Education and Science, Japan, a research grant for health sciences focusing on drug innovation for AIDS from the Japan Health Sciences Foundation, and a grant from the Program for the Promotion of Fundamental Studies in Health Sciences of the National Institute of Biomedical Innovation (NIBIO) of Japan.

REFERENCES

1. **Brenchley, J. M., D. A. Price, and D. C. Douek.** 2006. HIV disease: fallout from a mucosal catastrophe? Nat. Immunol. **7**:235–239.
2. **Brenchley, J. M., T. W. Schacker, L. E. Ruff, D. A. Price, J. H. Taylor, G. J. Beilman, P. L. Nguyen, A. Khoruts, M. Larson, A. T. Haase, and D. C. Douek.** 2004. $CD4^+$ T cell depletion during all stages of HIV disease occurs predominantly in the gastrointestinal tract. J. Exp. Med. **200**:749–759.
3. **Chase, A., Y. Zhou, and R. F. Siliciano.** 2006. HIV-1-induced depletion of $CD4^+$ T cells in the gut: mechanism and therapeutic implications. Trends Pharmacol. Sci. **27**:4–7.
4. **Gordon, S. N., N. R. Klatt, S. E. Bosinger, J. M. Brenchley, J. M. Milush, J. C. Engram, R. M. Dunham, M. Paiardini, S. Klucking, A. Danesh, E. A. Strobert, C. Apetrei, I. V. Pandrea, D. Kelvin, D. C. Douek, S. I. Staprans, D. L. Sodora, and G. Silvestri.** 2007. Severe depletion of mucosal $CD4^+$ T cells in AIDS-free simian immunodeficiency virus-infected sooty mangabeys. J. Immunol. **179**:3026–3034.
5. **Guadalupe, M., E. Reay, S. Sankaran, T. Prindiville, J. Flamm, A. McNeil, and S. Dandekar.** 2003. Severe $CD4^+$ T-cell depletion in gut lymphoid tissue during primary human immunodeficiency virus type 1 infection and substantial delay in restoration following highly active antiretroviral therapy. J. Virol. **77**:11708–11717.
6. **Igarashi, T., C. R. Brown, R. A. Byrum, Y. Nishimura, Y. Endo, R. J. Plishka, C. Buckler, A. Buckler-White, G. Miller, V. M. Hirsch, and M. A. Martin.** 2002. Rapid and irreversible $CD4^+$ T-cell depletion induced by the highly pathogenic simian/human immunodeficiency virus SHIV(DH12R) is systemic and synchronous. J. Virol. **76**:379–391.
7. **Igarashi, T., Y. Endo, G. Englund, R. Sadjadpour, T. Matano, C. Buckler, A. Buckler-White, R. Plishka, T. Theodore, R. Shibata, and M. A. Martin.** 1999. Emergence of a highly pathogenic simian/human immunodeficiency virus in a rhesus macaque treated with anti-CD8 mAb during a primary infection with a nonpathogenic virus. Proc. Natl. Acad. Sci. USA **96**:14049–14054.
8. **Joag, S. V., Z. Li, L. Foresman, E. B. Stephens, L.-J. Zhao, I. Adany, D. M. Pinson, H. M. McClure, and O. Narayan.** 1996. Chimeric simian/human immunodeficiency virus that causes progressive loss of $CD4^+$ T cells and AIDS in pig-tailed macaques. J. Virol. **70**:3189–3197.
9. **Kato, S., Y. Hiraishi, N. Nishimura, T. Sugita, M. Tomihama, and T. Takano.** 1998. A plaque hybridization assay for quantifying and cloning infectious human immunodeficiency virus type 1 virions. J. Virol. Methods **72**:1–7.
10. **Kozyrev, I. L., K. Ibuki, T. Shimada, T. Kuwata, T. Takemura, M. Hayami, and T. Miura.** 2001. Characterization of less pathogenic infectious molecular clones derived from acute-pathogenic SHIV-89.6p stock virus. Virology **282**: 6–13.
11. **Li, Q., L. Duan, J. D. Estes, Z. M. Ma, T. Rourke, Y. Wang, C. Reilly, J. Carlis, C. J. Miller, and A. T. Haase.** 2005. Peak SIV replication in resting memory $CD4^+$ T cells depletes gut lamina propria $CD4^+$ T cells. Nature **434**:1148–1152.
12. **Mattapallil, J. J., D. C. Douek, B. Hill, Y. Nishimura, M. Martin, and M. Roederer.** 2005. Massive infection and loss of memory $CD4^+$ T cells in multiple tissues during acute SIV infection. Nature **434**:1093–1097.
13. **Mehandru, S., M. A. Poles, K. Tenner-Racz, A. Horowitz, A. Hurley, C. Hogan, D. Boden, P. Racz, and M. Markowitz.** 2004. Primary HIV-1 infection is associated with preferential depletion of $CD4^+$ T lymphocytes from effector sites in the gastrointestinal tract. J. Exp. Med. **200**:761–770.
14. **Milush, J. M., J. D. Reeves, S. N. Gordon, D. Zhou, A. Muthukumar, D. A. Kosub, E. Chacko, L. D. Giavedoni, C. C. Ibegbu, K. S. Cole, J. L. Miamidian, M. Paiardini, A. P. Barry, S. I. Staprans, G. Silvestri, and D. L. Sodora.** 2007. Virally induced $CD4^+$ T cell depletion is not sufficient to induce AIDS in a natural host. J. Immunol. **179**:3047–3056.
15. **Miyake, A., Y. Enose, S. Ohkura, H. Suzuki, T. Kuwata, T. Shimada, S. Kato, O. Narayan, and M. Hayami.** 2004. The quantity and diversity of infectious viruses in various tissues of SHIV-infected monkeys at the early and AIDS stages. Arch. Virol. **149**:943–955.
16. **Miyake, A., K. Ibuki, Y. Enose, H. Suzuki, R. Horiuchi, M. Motohara, N. Saito, T. Nakasone, M. Honda, T. Watanabe, T. Miura, and M. Hayami.** 2006. Rapid dissemination of a pathogenic simian/human immunodeficiency virus to systemic organs and active replication in lymphoid tissues following intrarectal infection. J. Gen. Virol. **87**:1311–1320.
17. **Miyake, A., K. Ibuki, H. Suzuki, R. Horiuchi, N. Saito, M. Motohara, M. Hayami, and T. Miura.** 2005. Early virological events in various tissues of newborn monkeys after intrarectal infection with pathogenic simian human immunodeficiency virus. J. Med. Primatol. **34**:294–302.
18. **Motohara, M., K. Ibuki, A. Miyake, Y. Fukazawa, K. Inaba, H. Suzuki, K. Masuda, N. Minato, H. Kawamoto, T. Nakasone, M. Honda, M. Hayami, and T. Miura.** 2006. Impaired T-cell differentiation in the thymus at the early stages of acute pathogenic chimeric simian-human immunodeficiency virus (SHIV) infection in contrast to less pathogenic SHIV infection. Microbes Infect. **8**:1539–1549.
19. **Pandrea, I. V., R. Gautam, R. M. Ribeiro, J. M. Brenchley, I. F. Butler, M. Pattison, T. Rasmussen, P. A. Marx, G. Silvestri, A. A. Lackner, A. S. Perelson, D. C. Douek, R. S. Veazey, and C. Apetrei.** 2007. Acute loss of intestinal $CD4^+$ T cells is not predictive of simian immunodeficiency virus virulence. J. Immunol. **179**:3035–3046.
20. **Picker, L. J.** 2006. Immunopathogenesis of AIDS virus infection. Curr. Opin. Immunol. **18**:399–405.
21. **Picker, L. J., and D. I. Watkins.** 2005. HIV pathogenesis: the first cut is the deepest. Nat. Immunol. **6**:430–432.
22. **Reimann, K. A., J. T. Li, R. Veazey, M. Halloran, I. W. Park, G. B. Karlsson, J. Sodroski, and N. L. Letvin.** 1996. A chimeric simian/human immunodeficiency virus expressing a primary patient human immunodeficiency virus type 1 isolate *env* causes an AIDS-like disease after in vivo passage in rhesus monkeys. J. Virol. **70**:6922–6928.
23. **Shinohara, K., K. Sakai, S. Ando, Y. Ami, N. Yoshino, E. Takahashi, K. Someya, Y. Suzaki, T. Nakasone, Y. Sasaki, M. Kaizu, Y. Lu, and M. Honda.** 1999. A highly pathogenic simian/human immunodeficiency virus with genetic changes in cynomolgus monkey. J. Gen. Virol. **80**:1231–1240.
24. **Smit-McBride, Z., J. J. Mattapallil, M. McChesney, D. Ferrick, and S. Dandekar.** 1998. Gastrointestinal T lymphocytes retain high potential for cytokine responses but have severe $CD4^+$ T-cell depletion at all stages of simian immunodeficiency virus infection compared to peripheral lymphocytes. J. Virol. **72**:6646–6656.
25. **Veazey, R. S., M. DeMaria, L. V. Chalifoux, D. E. Shvetz, D. R. Pauley, H. L. Knight, M. Rosenzweig, R. P. Johnson, R. C. Desrosiers, and A. A. Lackner.** 1998. Gastrointestinal tract as a major site of $CD4^+$ T cell depletion and viral replication in SIV infection. Science **280**:427–431.
26. **Veazey, R. S., and A. A. Lackner.** 2004. Getting to the guts of HIV pathogenesis. J. Exp. Med. **200**:697–700.

Functional B7.2 and B7-H2 Molecules on Myeloma Cells Are Associated with a Growth Advantage

Taishi Yamashita,[1,3] Hideto Tamura,[1] Chikako Satoh,[1,4] Eiji Shinya,[2] Hidemi Takahashi,[2] Lieping Chen,[5] Asaka Kondo,[1] Takashi Tsuji,[3] Kazuo Dan,[1] and Kiyoyuki Ogata[1]

Abstract

Purpose: B7 family molecules expressed on antigen-presenting cells stimulate or inhibit normal immune responses. The aim of this study was to investigate whether functional B7.2 and B7-H2 molecules are expressed on myeloma cells and, if so, whether they are associated with pathophysiology in myeloma.

Experimental Design: The expression of B7.2 and B7-H2 molecules on normal plasma and neoplastic (myeloma) plasma cells was analyzed. The cell proliferation and immunomodulatory function of myeloma cells related to B7.2 and B7-H2 expression were examined.

Results: Human myeloma cell lines commonly expressed B7.2 and B7-H2 molecules. B7.2 expression on plasma cells was more common in myeloma patients ($n = 35$) compared with that in patients with monoclonal gammopathy of unknown significance ($n = 12$) or hematologically normal individuals ($n = 10$). Plasma cells expressing B7-H2 were observed in myeloma patients alone, although rarely. Patients whose myeloma cells showed high B7.2 expression were more anemic and thrombocytopenic than other myeloma patients. The expression of these molecules was induced or augmented by cultivating myeloma cells with autologous stroma cells or tumor necrosis factor-α, a key cytokine in myeloma biology. Cell proliferation was more rapid in the $B7.2^+$ and $B7\text{-}H2^+$ populations compared with the $B7.2^-$ and $B7\text{-}H2^-$ populations, respectively, in the human myeloma cell lines examined. B7.2 and B7-H2 molecules on myeloma cells induced normal $CD4^+$ T cells to proliferate and produce soluble factors, including interleukin-10 that stimulate myeloma cell proliferation.

Conclusions: Functional B7.2 and B7-H2 molecules detected on myeloma cells may be involved in the pathophysiology of myeloma.

Multiple myeloma (MM) is a virtually incurable hematologic malignancy characterized by monoclonal growth of plasma cells (myeloma cells). In addition to the well-known deficiency in B-cell immunity, T-cell dysfunction, such as reduced cytotoxic activity (1) and reduced responsiveness to interleukin 2 (IL-2; refs. 2, 3), has been reported, which may weaken antitumor immune responses in MM patients. The interaction between myeloma cells and bone marrow (BM) stroma cells stimulates the production of a variety of cytokines that are involved in the pathophysiology of MM (4, 5). Those include IL-6, IL-10, and tumor necrosis factor-α (TNF-α), which stimulate myeloma cell growth (6–9). An interesting aspect is that both IL-10 and TNF-α have an immunomodulating function, including inhibition of CTLs (10–12).

The B7 family molecules play an important role in the immune response by costimulating or coinhibiting T cells via antigen–T-cell receptor interactions (13–16). Interactions between B7.1/B7.2 ligands on professional antigen-presenting cells and CD28/CTLA-4 receptors on T cells represent a classic pathway and control antigen-specific T-cell proliferation, anergy, and survival. B7-H2 is another B7 family molecule induced by TNF-α (17). The binding of B7-H2 to the inducible costimulatory receptor (ICOS), a counterreceptor, induces T cells to proliferate and secrete both Th1 and Th2 cytokines, such as IFN-γ and IL-4 but not the potent Th1 cytokine IL-2 (18). Furthermore, the B7-H2-ICOS signal induces IL-10 production, which plays an important role in reducing immune responses (19, 20). B7 family molecules are expressed not only on professional antigen-presenting cells but also on some tumor cells and the latter may modulate antitumor immunity in hosts. For example, we detected the expression of B7.2 and B7-H2 molecules on blasts from patients with acute myeloid leukemia and showed that these molecules on acute myeloid

Authors' Affiliations: [1]Division of Hematology, Department of Medicine and [2]Department of Microbiology and Immunology, Nippon Medical School, Tokyo, Japan; [3]Department of Biological Science and Technology, Tokyo University of Science, Chiba, Japan; [4]Department of Bioregulation, Institute of Development and Aging Science, Nippon Medical School, Kawasaki, Japan; and [5]Department of Dermatology, Department of Oncology and Institute for Cell Engineering, Johns Hopkins University School of Medicine, Baltimore, Maryland

Received 2/24/08; revised 10/21/08; accepted 10/25/08.

Grant support: A Grant-in-Aid for Scientific Research from the Japan Society for the Promotion of Science (no. 20591157).

The costs of publication of this article were defrayed in part by the payment of page charges. This article must therefore be hereby marked *advertisement* in accordance with 18 U.S.C. Section 1734 solely to indicate this fact.

Note: Supplementary data for this article are available at Clinical Cancer Research Online (http://clincancerres.aacrjournals.org/).

Requests for reprints: Hideto Tamura, Division of Hematology, Department of Medicine, Nippon Medical School, 1-1-5 Sendagi, Bunkyo-ku, Tokyo 113-8603, Japan. Phone: 81-3-3822-2131; Fax: 81-3-5685-1793; E-mail: tam@nms.ac.jp.

doi:10.1158/1078-0432.CCR-08-0501

Translational Relevance

Multiple myeloma (MM) is a virtually incurable hematologic malignancy. Therefore, research that could result in improved MM treatment and/or a breakthrough in our understanding of this disease is very important. This article shows that myeloma cells from a substantial number of MM patients express functional B7.2 or B7-H2 molecules. Furthermore, it provides evidence that these molecules on myeloma cells may be involved in the pathophysiology of the disease. It is anticipated that these data will be translated into a new therapeutic strategy for MM.

leukemia blasts inhibited anti-acute myeloid leukemia immunity *in vitro* and were associated with poor patient prognosis (21). In MM, data on B7 family molecules are lacking. To the best of our knowledge, only one study examined this topic. Pope et al. (22) observed that MM patients whose tumor cells expressed B7.2 molecules had a poor prognosis. However, they did not examine whether the B7.2 molecules on myeloma cells were functional. Here, we investigated whether functional B7.2 and B7-H2 molecules are expressed on myeloma cells and, if so, whether these B7 molecules are associated with pathophysiology in MM.

Materials and Methods

Cell lines. Eleven human myeloma cell lines (HMCL), KMM-1, KMS-11, KMS-12BM, KMS-12PE, KMS-18, KMS-20, KMS-26, KMS-27, KMS-28BM, KMS-28PE, and KMS-34, were kindly provided by Dr. Otsuki (Kawasaki Medical School, Okayama, Japan). PCM6 cells were obtained from the Riken Cell Bank, and RPMI8226 and U266 cells were from the American Type Culture Collection. PCM6 cells were maintained in McCoy's 5A modified medium (Life Technologies) containing 20% FCS and 3 ng/mL of recombinant IL-6 (Kirin Brewery Co.). The other cells were maintained in complete medium, i.e., RPMI 1640 supplemented with 10% FCS and 2 mmol/L L-glutamine. In experiments examining the effects of cytokines on these cells, TNF-α

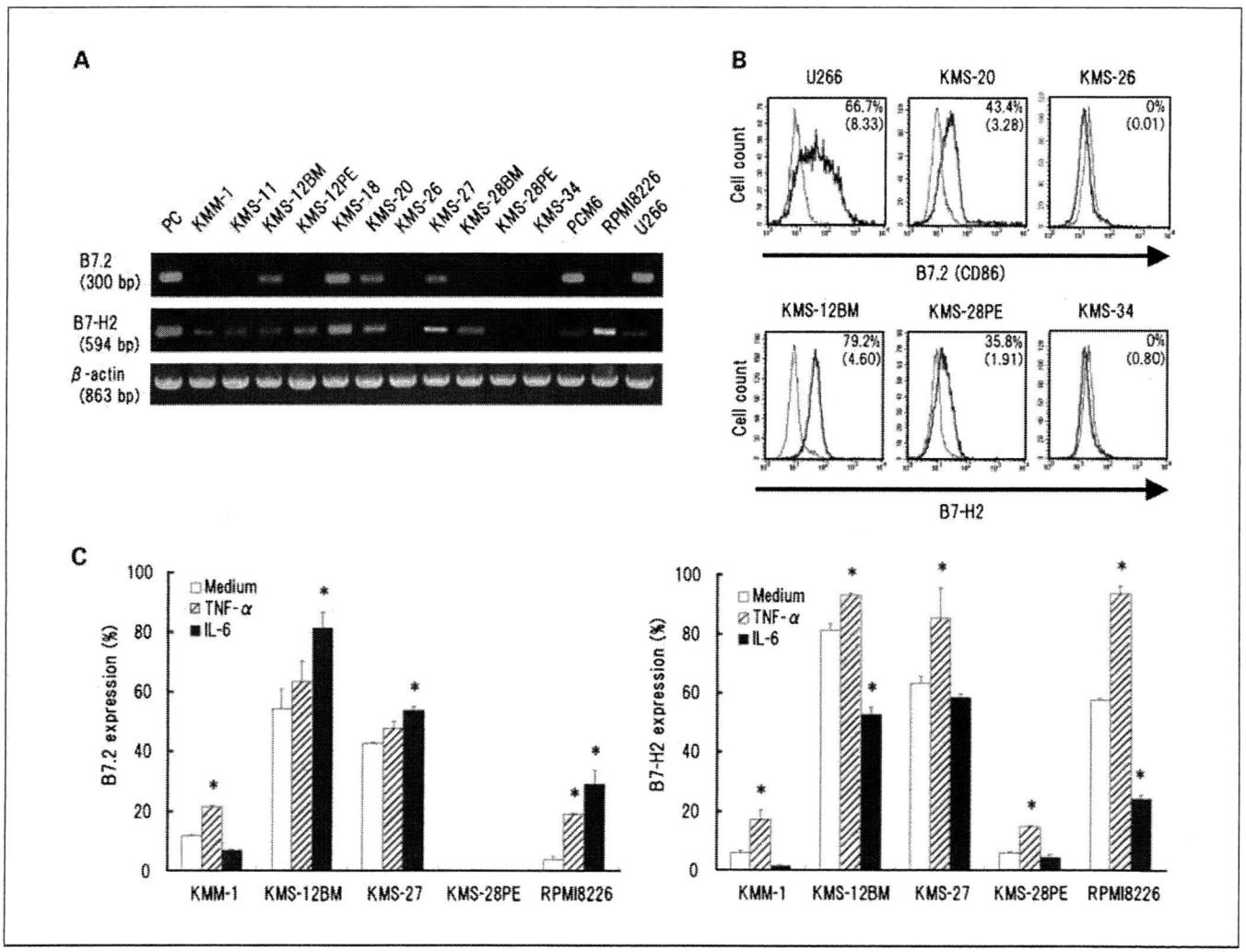

Fig. 1. *A*, B7.2 and B7-H2 mRNA expression analyzed using reverse transcription-PCR in 14 HMCLs. Equal amounts of cDNA from each cell line were amplified using primers specific for B7.2, B7-H2, and β-actin. *B*, representative flow cytometry analyses of the B7.2 and B7-H2 expression in HMCLs. Bold curves, staining with anti-B7.2 or anti-B7-H2 mAb; thin curves, staining with isotype-matched control immunoglobulin. Data are expressed in the percentages of positive cells and in relative mean fluorescence intensity (*numbers in parentheses*). *C*, effects of TNF-α and IL-6 on B7.2 and B7-H2 expression in HMCLs. Columns, mean of three independent experiments; bars, SD. Medium, no cytokine was added. *, $P < 0.05$, significantly different from Medium.

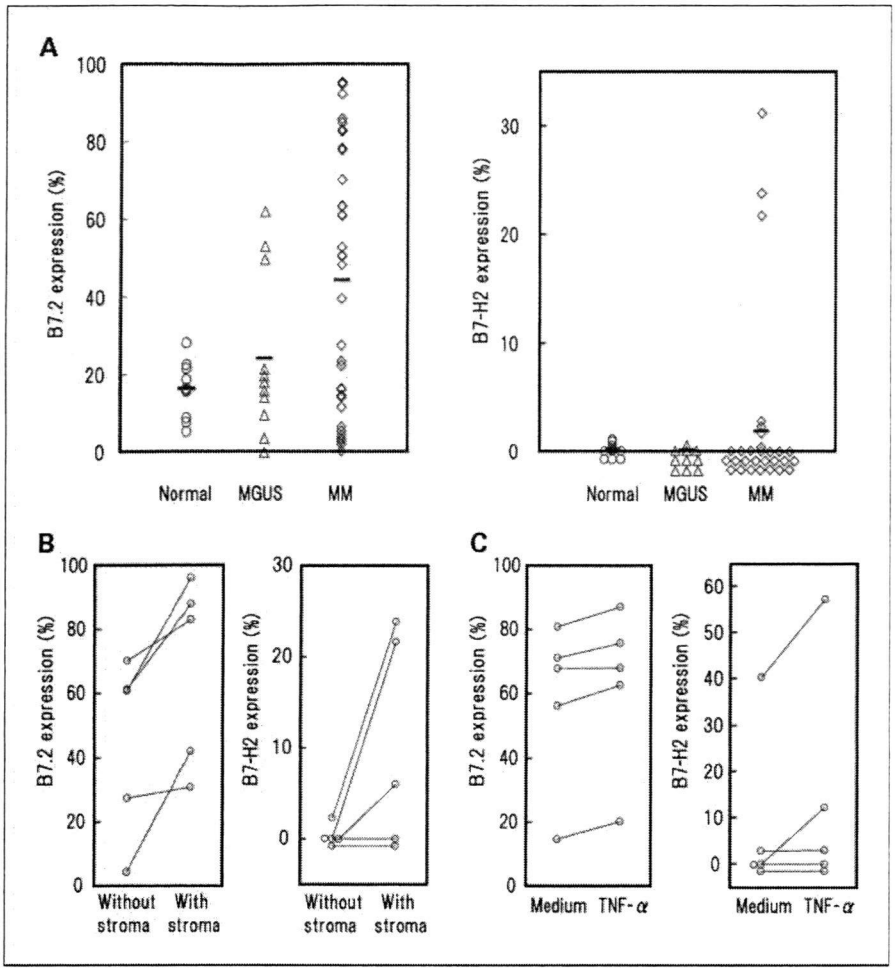

Fig. 2. *A*, percentages of B7.2$^+$ and B7-H2$^+$ plasma cells among all plasma cells in 10 hematologically normal individuals and 12 monoclonal gammopathy of unknown significance and 35 MM patients determined using flow cytometry. Horizontal bars, mean. Effects of autologous stroma cells (*B*) and TNF-α (*C*) on B7.2 and B7-H2 expression on myeloma cells from patients.

(500 units/mL; PeproTech), IL-10 (10 ng/mL; MBL), or IL-6 (10 ng/mL) were added to the cultures. The cell number was counted using the trypan blue dye-exclusion method.

In some experiments, B7.2$^+$, B7.2$^-$, B7-H2$^+$, or B7-H2$^-$ KMS-27 cells were purified with FACSVantage (Becton Dickinson) as described previously (23).

Patients, hematologically normal individuals, and cell preparation. BM samples were obtained from individuals who underwent BM aspiration for diagnostic purposes after obtaining written informed consent. They included 35 MM patients [4 stage I and 31 stage III according to the definition of Durie and Salmon (24)], 12 patients with monoclonal gammopathy of unknown significance, and 10 hematologically normal individuals. All BM samples from MM patients were obtained at the initial diagnosis, except for those from 6 patients, 2 of whose samples showed that they were refractory to conventional chemotherapy and 4 of whose samples were in the plateau phase according to the standard definition. Diagnoses were made according to the WHO classification. Mononuclear cells were separated from BM samples with Histopaque (Sigma) density centrifugation. These cells were used immediately or cryopreserved in liquid nitrogen until use. In cell samples from hematologically normal individuals, CD19-positive cells were enriched from BM mononuclear cells using magnetic cell sorting (Miltenyi Biotec; ref. 23) to ensure plasma cell identification in flow cytometry (25). This study was approved by the institutional review board of Nippon Medical School.

Stroma cells were prepared as follows. BM mononuclear cells from MM patients (2×10^6/mL) were plated in 6-well plates in complete medium. The cultures were fed weekly by removing 75% of the medium and adding fresh medium to make up the same volume. After the cultivated cells became adherent, stromal cell shaped, positive for mesenchymal stem cell markers (CD44 and CD90), and negative for hematopoietic markers (CD34, CD45, and CD11b), they were used as stroma cells (26). In experiments inducing B7.2 and B7-H2 expression, mononuclear cells were cultured in complete medium on autologous stroma cells for 3 wk or with TNF-α (500 units/mL) for 2 d.

Reverse transcription-PCR. Total RNA extracted from each HMCL was reverse transcribed with Superscript II Reverse transcriptase (Invitrogen) using random hexamers. PCR amplification was done using the primer sets for B7.2 and B7-H2 and PCR conditions previously described (21).

Flow cytometry. Immunophenotyping was done with FACScan (Becton Dickinson; refs. 21, 27). Briefly, after blocking with human immunoglobulin, patient BM samples were stained with anti-CD38 monoclonal antibody (mAb) labeled with FITC and phycoerythrin-labeled anti-B7.2 (Becton Dickinson) or anti-B7-H2 mAb (e-Bioscience). Plasma cells were identified by a high expression of CD38 molecules (22). We also confirmed that the identified plasma cells expressed another plasma cell marker, CD138 (Becton Dickinson). Examples of flow cytometry analysis are shown in Supplementary Fig. S1. HMCLs were single stained with FITC/phycoerythrin–conjugated mAbs against lymphocyte function–associated antigen-1 (LFA-1), intercellular adhesion molecule-1 (ICAM-1; Beckman Coulter), very late antigen-4, vascular cell adhesion molecule-1 (Becton Dickinson), B7.2, and B7-H2.

Cell cycle analysis. After blocking with human immunoglobulin, HMCLs were stained with purified mouse anti-B7.2 or anti-B7-H2

mAbs. The cells were washed and further incubated with FITC-conjugated antimouse IgG (Biosource). Then, the cells were fixed with 70% ethanol at 4°C for 3 h. The fixed cells were washed and resuspended in 100 μL of PBS and 1 μg of RNase (Qiagen) containing 0.1 mg/mL of propidium iodide (Sigma). The cell cycle profiles of B7.2$^+$, B7.2$^-$, B7-H2$^+$, and B7-H2$^-$ HMCLs were analyzed using flow cytometry.

Colony-forming assay. Purified B7.2$^+$, B7.2$^-$, B7-H2$^+$, and B7-H2$^-$ cells (1×10^3 per culture dish) were cultured in MethoCult H4230 methylcellulose medium (StemCell Technologies; ref. 23). Colonies (aggregates of 50 or more cells) were scored on day 14 of culture.

Mixed lymphocyte-myeloma reaction. CD4$^+$ T cells (purity > 95%) were prepared from peripheral blood of healthy volunteers on magnetic cell sorting columns (21). These cells (1×10^5) were cocultured with irradiated (20,000 rad) myeloma cells (1×10^5) expressing both B7.2 and B7-H2 molecules in microtiter wells for 5 d. Antagonistic mAbs (10 μg/mL) against B7.2 and ICOS (e-Bioscience) were added to the cultures to block the B7.2-CD28 and B7-H2-ICOS pathways, respectively. During the final 18 h of culture, [^{3}H]thymidine (1 μCi/well) was added to determine T-cell proliferation. All samples were assayed at least in quadruplicate.

In some experiments, culture supernatants of mixed lymphocyte-myeloma reaction (MLMR) were collected on day 5 of culture. The

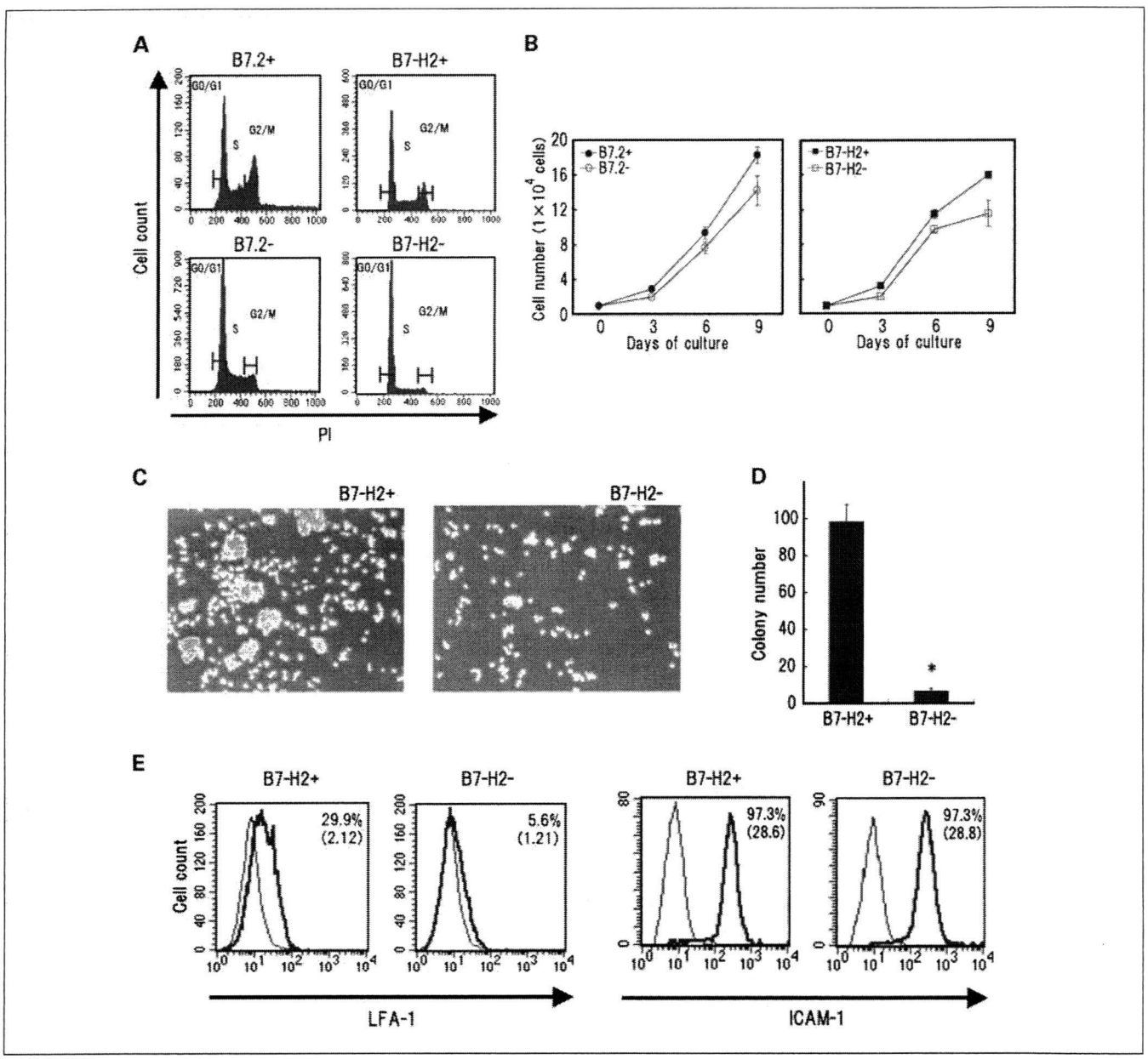

Fig. 3. *A,* cell cycle analyses of B7.2$^+$ or B7.2$^-$ KMS-27 cells (*left*) and of B7-H2$^+$ or B7-H2$^-$ KMS-27 cells (*right*). Each cell population was gated and analyzed in flow cytometry. Analysis on at least 10,000 events for each sample. The cell cycle data were reproducible when B7-H2$^+$ and B7-H2$^-$ KMS-27 cells isolated using FACSVantage were analyzed (data not shown). *B,* proliferation of isolated B7.2$^+$ or B7.2$^-$ KMS-27 cells and B7-H2$^+$ or B7-H2$^-$ KMS-27 cells. Points, mean of three independent experiments; bars, SD. *C,* photomicrographs of purified B7-H2$^+$ and B7-H2$^-$ KMS-27 cells during exponential cell growth in culture. *D,* number of colonies (defined as aggregates composed of 20 or more cells) formed by purified B7-H2$^+$ and B7-H2$^-$ cells on day 7 of culture. Columns, mean of three independent triplicate cultures; bars, SD. *, $P < 0.01$ compared with the data of B7-H2$^+$. *E,* representative flow cytometry analyses of LFA-1 and ICAM-1 expression on B7-H2$^+$ and B7-H2$^-$ KMS-27 cells. Bold curves, staining with anti – LFA-1 or anti – ICAM-1 mAb; thin curves, staining with isotype-matched control immunoglobulin. Data are expressed in percentages of positive cells and in relative mean fluorescence intensity (*numbers in parentheses*).

concentrations of IFN-γ, IL-2, IL-4, and IL-10 in the supernatants were measured with sandwich ELISA kits (eBioscience).

Coculture using a transwell system. KMS-27 (1×10^4) cells were plated onto a transwell membrane insert (Nunc) placed above the culture containing normal $CD4^+$ T cells (1×10^5) with or without irradiated KMS-27 cells (1×10^5). Antihuman IL-10 polyclonal antibody (R&D Systems), anti-B7.2, and/or anti-ICOS mAbs were added to the lower cultures to neutralize their biological activities. After 5 d of culture, KMS-27 cells above the insert were harvested and counted using the trypan blue dye-exclusion method.

Statistical analysis. Differences between two groups of data were determined with the χ^2 test and Student's *t* test for categorical and continuous variables, respectively, unless otherwise stated. The Mann-Whitney *U* test was used for two groups of data with continuous nonparametric variables. A *P* value of <0.05 was considered significant.

Results

Expression and induction of B7.2 and B7-H2 molecules on HMCLs. First, we analyzed the expression of B7.2 and B7-H2 molecules on HMCLs. Seven and 11 of 14 HMCLs expressed high levels of B7.2 and B7-H2 mRNA, respectively (Fig. 1A). These results were consistent with the protein expression analyzed using flow cytometry (Fig. 1B; Supplementary Table S1): The expression of B7.2 and B7-H2 molecules was detected in 7 (50.0%) and 9 (64.3%) HMCLs, respectively. Next, we examined whether cytokines, i.e., TNF-α, IL-6, or IL-10, affect B7.2 and B7-H2 expression in five HMCLs. TNF-α up-regulated the expression of both molecules in almost all cell lines examined. Meanwhile, IL-6 up-regulated B7.2 expression in three of five HMCLs and down-regulated B7-H2 expression in two of five HMCLs (Fig. 1C). IL-10 did not affect the expression of these molecules (data not shown).

Expression and induction of B7.2 and B7-H2 molecules in myeloma patients. Using flow cytometry, we examined the expression of B7.2 and B7-H2 molecules on fresh plasma cells. The percentages of $B7.2^+$ cells in plasma cells were much higher in MM patients than those in monoclonal gammopathy of unknown significance patients or in hematologically normal individuals (Fig. 2A, *left*; MM versus monoclonal gammopathy of unknown significance, $P = 0.0318$; MM versus normals, $P = 0.0145$; Mann-Whitney *U* test). When MM patients were divided into two groups using various cutoff percentages of B7.2 positivity, those in whom >40% of myeloma cells expressed B7.2 ($n = 18$, called $B7.2^{high+}$ MM patients in this article) showed significantly lower levels of hemoglobin and platelets compared with other MM patients ($B7.2^{-/low}$ MM patients in this article, $n = 17$; Supplementary Table S2). Although there was no difference in survival between the two groups of patients (data not shown), both patients refractory to chemotherapy were in the $B7.2^{high+}$ group and all four patients in the plateau phase were in the $B7.2^{-/low}$ group. Meanwhile, B7-H2 expression on plasma cells was clearly documented only in three MM patients. The disease of these three patients was intractable: one patient had plasma cell leukemia and the other two had chemotherapy-resistant MM. In our cohort of patients, BM cells from only two MM patients were analyzed for B7.2 and B7-H2 expression in different disease statuses at the initial diagnosis and at the stage of refractory disease. The expression of these molecules on myeloma cells was augmented at the refractory stage in both patients, except for B7-H2 expression in one patient in whom B7-H2 was not detected at either time point (Supplementary Table S3). All of the above findings support the idea that these molecules may be associated with disease progression in MM, although the clinical evidence remains insufficient for the B7-H2 molecule because of the rarity of B7-H2–positive patients.

Next, we examined whether stroma cells and TNF-α, both important for myeloma cell proliferation *in vivo*, modulate the expression of B7.2 and B7-H2 on myeloma cells from MM patients. B7.2 or B7-H2 expression on myeloma cells from >50% of patients examined was up-regulated after the cells were cultivated with autologous stroma cells or TNF-α (Fig. 2B and C).

Cell cycle and proliferation of myeloma cells based on B7.2 and B7-H2 expression. Based on the above data, we speculated that B7.2 or B7-H2 expression on myeloma cells was associated with their proliferative potential. When KMS-27 cells that did or did not express these B7 family molecules were analyzed, $B7.2^+$ and $B7\text{-}H2^+$ cells had significantly fewer $G_0\text{-}G_1$ phase cells and more G_2-M phase cells compared with $B7.2^-$ and $B7\text{-}H2^-$ cells, respectively (Fig. 3A; Table 1). Consistent with these results, the $B7.2^+$ and $B7\text{-}H2^+$ KMS-27 cells proliferated more rapidly in liquid cultures and formed more colonies in semisolid cultures compared with the $B7.2^-$ and $B7\text{-}H2^-$ KMS-27 cells, respectively (Fig. 3B; Supplementary Table S4). The same growth advantage of myeloma cells expressing B7.2 and B7-H2 molecules was also documented in all other HMCLs examined (Table 1; Supplementary Table S4; Supplementary Fig. S2).

We then examined whether myeloma cells have a growth advantage when the cells are induced to express B7.2 and B7-H2 molecules. When RPMI8226 cells, for which B7.2 and B7-H2 expression is inducible by TNF-α as shown in Fig. 1C, were treated with TNF-α, the cell cycle of the cells was clearly

Table 1. Cell cycling of HMCLs as a function of B7.2 and B7-H2 expression

Cell fraction in HMCLs	Cell cycle		
	$G_0\text{-}G_1$	S	G_2-M
KMS-27 cells			
$B7.2^+$	52.8 ± 0.9*	19.7 ± 0.1	27.6 ± 0.9*
$B7.2^-$	80.8 ± 1.6	16.0 ± 1.5	3.7 ± 0.4
$B7\text{-}H2^+$	53.7 ± 1.4*	18.6 ± 2.2	28.0 ± 0.9*
$B7\text{-}H2^-$	78.5 ± 0.8	17.5 ± 0.8	4.1 ± 1.3
KMS-20 cells			
$B7.2^+$	42.5 ± 0.7*	20.0 ± 0.1*	37.7 ± 0.8*
$B7.2^-$	74.2 ± 1.0	13.7 ± 0.6	12.3 ± 0.3
$B7\text{-}H2^+$	43.4 ± 1.1*	26.9 ± 0.4*	30.2 ± 0.6*
$B7\text{-}H2^-$	81.5 ± 0.9	13.4 ± 0.7	4.8 ± 0.3
U266 cells			
$B7.2^+$	49.5 ± 4.0*	23.7 ± 1.6	25.7 ± 3.8*
$B7.2^-$	65.0 ± 2.7	21.2 ± 0.5	13.9 ± 1.7
RPMI8226 cells			
$B7\text{-}H2^+$	39.5 ± 0.9*	33.1 ± 2.2*	26.9 ± 4.1*
$B7\text{-}H2^-$	64.4 ± 3.0	25.8 ± 2.4	9.3 ± 2.1

NOTE: Mean ± SD of three independent experiments. $B7\text{-}H2^+$ and $B7.2^+$ fractions in U266 and RPMI8226 cells, respectively, were sparse and thus were not analyzed.
*Significant difference ($P < 0.05$) when data of each cell cycle phase were compared between $B7.2^+$ (or $B7\text{-}H2^+$) and $B7.2^-$ (or $B7\text{-}H2^-$) cell fractions in each HMCL.

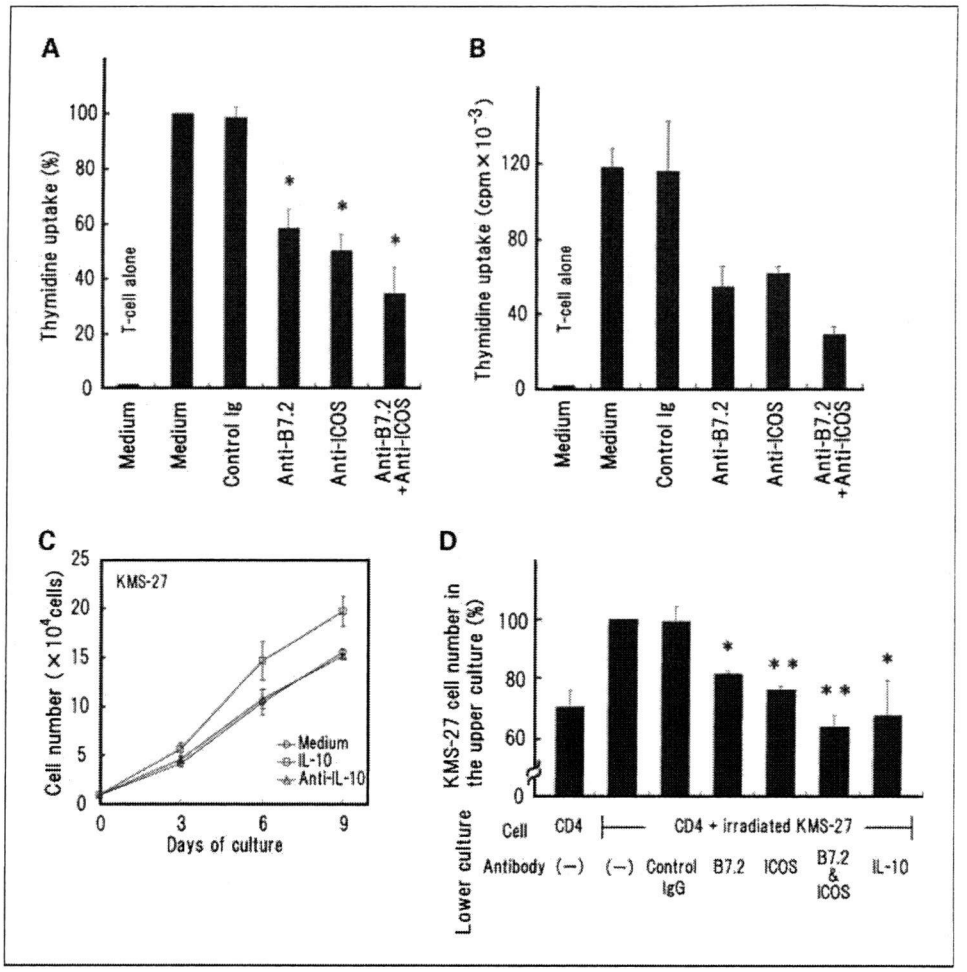

Fig. 4. *A*, MLMR. Normal CD4$^+$ Tcells were cultured with (*five columns, right*) or without (*first column, left*) irradiated KMS-27 cells that expressed B7.2 and B7-H2. Effects of anti-B7.2 and anti-ICOS blocking mAbs on CD4$^+$ T-cell proliferation were examined in this assay. Columns, mean of three independent triplicate cultures, in which the second column from the left was defined as 100%; bars, SD. Medium, no antibody was added. *, $P < 0.01$ compared with the data for control immunoglobulin. *B*, MLMR done using the same method as described in *A*, except that irradiated patient MM cells expressing B7.2 and B7-H2 were used instead of KMS-27 cells. Columns, mean of triplicate cultures; bars, SD. *C*, kinetics of KMS-27 cell proliferation. The cells were cultured in medium alone or in medium containing anti – IL-10 neutralizing antibody or recombinant IL-10. Points, mean of three independent experiments; bars, SD. *D*, cultures using a transwell system. KMS-27 cells were plated onto a transwell membrane insert, which was placed above the culture containing CD4$^+$ Tcells alone (*first columns, left*) or CD4$^+$ Tcells with irradiated KMS-27 cells (*six columns, right*). Blocking antibodies to B7.2, ICOS, and/or IL-10 were added to the lower cultures and their effects on KMS-27 cell proliferation in the upper cultures were examined. Columns, mean of three independent triplicate cultures, in which the second column from the left was defined as 100%; bars, SD. *, $P < 0.05$; **, $P < 0.01$ compared with the data for control immunoglobulin.

stimulated (Supplementary Table S5). Furthermore, when 293T cells (a human kidney cell line suitable for efficient transfection experiments) were transfected with either B7.2 or B7-H2 gene or Mock, B7.2 or B7-H2 gene induction induced cell cycle activation (Supplementary Table S6).

We noted that even in liquid culture, B7-H2$^+$ KMS-27 cells often formed colonies during exponential cell growth (Fig. 3C): There were many more colonies of B7-H2$^+$ cells compared with B7-H2$^-$ cells in liquid culture (Fig. 3D). Meanwhile, there was no difference in colony formation in liquid culture between B7.2$^+$ and B7.2$^-$ KMS-27 cells (data not shown). Therefore, we investigated the expression of adhesion molecules (LFA-1, ICAM-1, very late antigen-4, vascular cell adhesion molecule-1), which might mediate the adhesion of myeloma cells to BM stroma cells and induce drug resistance (28, 29) on B7-H2$^+$ and B7-H2$^-$ KMS-27 cells. The expression levels of LFA-1 were much higher on B7-H2$^+$ KMS-27 cells compared with those on B7-H2$^-$ KMS-27 cells, although there was no difference in the expression of the other adhesion molecules (Fig. 3E).

Interaction between B7.2$^+$ and B7-H2$^+$ myeloma cells and CD4$^+$ T cells confers a myeloma growth advantage. In the MLMR, normal CD4$^+$ T cells were cultured with KMS-27 cells with or without anti-B7.2 and anti-ICOS mAbs. In a 5-day culture, either the anti-B7.2 or anti-ICOS mAb decreased the proliferation of CD4$^+$ T cells and the combined use of these antibodies resulted in the maximum decrease (Fig. 4A). In other words, both B7.2 and B7-H2 molecules on KMS-27 cells stimulated CD4$^+$ T-cell proliferation. The same result was obtained when fresh myeloma cells obtained from a plasma cell leukemia patient and expressing both B7.2 and B7-H2 molecules were used in the MLMR (Fig. 4B).

It was reported that B7.2 enhanced the production of Th1 and Th2 cytokines and that B7-H2 did not contribute to IL-2 induction (18, 19, 30). Consistent with these results, in MLMR using KMS-27 cells and CD4$^+$ T cells, the mAb against B7.2 decreased the production of IL-10 as well as IFN-γ and IL-2. Meanwhile, the mAb against ICOS decreased the production of IL-10 and IFN-γ but not that of IL-2 (Supplementary Fig. S3). IL-4 was not detected in the supernatant of MLMR. The finding that both B7.2 and B7-H2 molecules on myeloma cells enhanced IL-10 production is particularly interesting because IL-10 not only reduces the antitumor immune response in general but also is a growth factor for myeloma cells.

Then, we examined whether soluble factors including IL-10 produced by the interaction between myeloma cells and CD4$^+$ cells stimulate myeloma cell growth *in vitro*. First, we confirmed that when anti-IL-10 neutralizing antibody or control immunoglobulin was added to the KMS-27 cell culture, cell proliferation was not affected (Fig. 4C; data for control immunoglobulin are not shown). Furthermore, IL-10 was not detected in the supernatant of KMS-27 cell culture when examined using ELISA (data not shown). Therefore, KMS-27

cells themselves did not produce IL-10, but their proliferation was stimulated by exogenous IL-10 (Fig. 4C). Next, we cocultured using a transwell system, in which KMS-27 cells were plated onto a transwell membrane insert placed above the culture containing normal $CD4^+$ T cells with or without irradiated KMS-27 cells. The presence of irradiated KMS-27 cells in the lower cultures, compared with their absence, stimulated KMS-27 cell proliferation in the upper cultures (Fig. 4D, *two columns on the left*). Furthermore, this growth-promoting effect resulting from the $CD4^+$ T cell-irradiated KMS-27 cell interaction was eliminated partially or completely by adding anti-B7.2 mAb, anti-ICOS mAb, and/or anti-IL-10 neutralizing mAb to the lower cultures (Fig. 4D, *four columns on the right*). These results suggest that B7.2 or B7-H2 molecules on KMS-27 cells enhance $CD4^+$ T-cell proliferation and stimulate them to produce soluble factors, one of which, IL-10, enhances KMS-27 cell proliferation.

Discussion

The B7 family molecules stimulate or inhibit immune responses by costimulating or coinhibiting T cells. For example, in a mouse tumor model, B7-H2–expressing tumors increase the proliferation of tumor-specific CTLs (31). Meanwhile, the B7-H2-ICOS signal down-regulates the immune response in experimental animal models of autoimmune disease or acute graft-versus-host disease (32–34).

This study showed that the B7.2 expression levels on plasma cells were higher in MM patients compared with those in monoclonal gammopathy of unknown significance patients and hematologically normal individuals, and B7-H2 expression was detected in three MM patients alone but not in any monoclonal gammopathy of unknown significance patient or hematologically normal individual. Next, the expression of B7.2 and B7-H2 on MM cells was induced or enhanced by coculture with autologous stroma cells or by stimulation with TNF-α. Furthermore, myeloma cells expressing B7.2 and B7-H2 had increased cell cycling and more potential for proliferation. Finally, B7.2 and B7-H2 molecules on myeloma cells enhanced $CD4^+$ T-cell proliferation and stimulated them to produce soluble factors, one of which, IL-10, further stimulates the proliferation of myeloma cells.

B7.2 and B7-H2 molecules on myeloma cells were also involved in the production of other cytokines, IFN-γ and IL-2, which are known to enhance antitumor immune responses in general (35, 36). However, we and others observed that the expression of these molecules on acute myelogenous leukemia cells was associated with poor patient prognosis (21, 37). Similarly, lymphoma cells expressing B7.2 are associated with poor prognosis in a mouse lymphoma model (38). The effects of IFN-γ and IL-2, the production of which might be induced by B7.2 and B7-H2 molecules on myeloma cells, on the immunology and clinical behavior of MM should be clarified in further studies.

TNF-α, an immunomodulatory cytokine capable of inhibiting CTLs, is produced by the interaction between BM stroma cells and myeloma cells (39). It was shown that TNF-α directly stimulates myeloma cell growth *in vitro* and that serum TNF-α levels are higher in advanced-stage compared with early-stage MM patients (6, 7, 40). Based on our data presented here, we speculate that the TNF-α–induced growth advantage in myeloma may be, at least in part, associated with the induction of B7.2 and B7-H2 molecule expression on myeloma cells. The mechanism underlying the finding that myeloma cells expressing B7.2 and B7-H2 show increased cell cycling and greater potential to proliferate remains unknown. To the best of our knowledge, one previous report observed a similar phenomenon. Ghebeh et al. reported that high B7-H1 expression was correlated with high Ki-67 expression in tumor cells in breast cancer patients (41). In addition to this intrinsic advantage in cell proliferation of $B7.2^+$ and $B7\text{-}H2^+$ myeloma cells, these cells may obtain a further growth advantage by inducing the production of the myeloma-stimulatory cytokine IL-10 by $CD4^+$ T cells. It is well known that IL-10 inhibits the generation of tumor-specific CTLs (11, 12). We also confirmed that IL-10 inhibited the generation of KMS-27–specific CTLs *in vitro* (data not shown). This IL-10–mediated effect probably contributes further to myeloma cell growth. The above cascade of events is illustrated in Fig. 5. The IL-10 production induced by B7.2 and B7-H2 molecules is not myeloma specific because we observed that that AML cells expressing B7.2 and B7-H2 induced IL-10 production by $CD4^+$ T cells *in vitro*. It would be interesting to determine how broadly this mechanism works in a variety of human neoplasia.

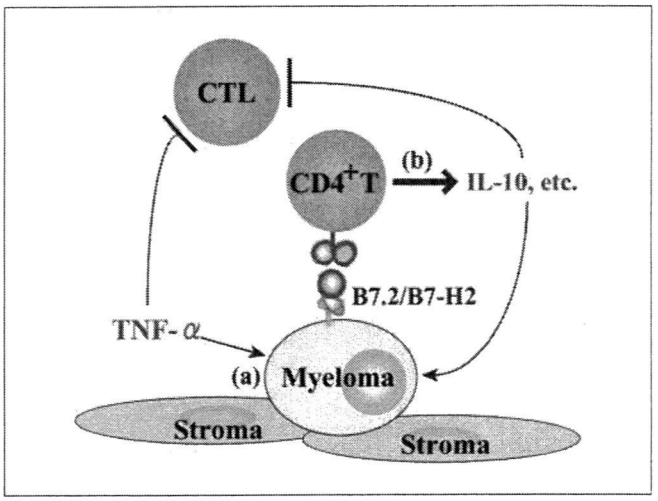

Fig. 5. New insight into myeloma biology based on the present data. *A*, in the BM environment, TNF-α and stromal cell contact induce B7.2 and B7-H2 molecule expression on myeloma cells. $B7.2^+$ and $B7\text{-}H2^+$ myeloma cells gain an intrinsic proliferative advantage. TNF-α also inhibits myeloma-specific CTLs. *B*, the B7.2 and B7-H2 molecules on myeloma cells induce $CD4^+$ T cells to produce soluble factors, one of which, IL-10, stimulates myeloma cell proliferation and inhibits myeloma-specific CTLs.

The occurrence of immunologic derangement in MM supports the notion that modulation or normalization of this derangement would be beneficial for MM patients. Thalidomide and its analogues (e.g., lenalidomide), which have a variety of imunomodulatory activities, including potent inhibition of TNF-α production and stimulation of Th-1 immunity (42, 43), are effective in the treatment of MM patients. We speculate that full clarification of immunology in MM is the basis on which more specific, targeted therapy will be developed.

Disclosure of Potential Conflicts of Interest

No potential conflicts of interest were disclosed.

References

1. Massaia M, Dianzani U, Bianchi A, Camponi A, Boccadoro M, Pileri A. Defective generation of alloreactive cytotoxic T lymphocytes (CTL) in human monoclonal gammopathies. Clin Exp Immunol 1988; 73:214–8.
2. Cook G, Campbell JD, Carr CE, Boyd KS, Franklin IM. Transforming growth factor β from multiple myeloma cells inhibits proliferation and IL-2 responsiveness in T lymphocytes. J Leukoc Biol 1999;66:981–8.
3. Campbell JD, Cook G, Robertson SE, et al. Suppression of IL-2-induced T cell proliferation and phosphorylation of STAT3 and STAT5 by tumor-derived TGF β is reversed by IL-15. J Immunol 2001;167:553–61.
4. Hideshima T, Podar K, Chauhan D, Anderson KC. Cytokines and signal transduction. Best Pract Res Clin Haematol 2005;18:509–24.
5. Yasui H, Hideshima T, Richardson PG, Anderson KC. Novel therapeutic strategies targeting growth factor signalling cascades in multiple myeloma. Br J Haematol 2006;132:385–97.
6. Borset M, Waage A, Brekke OL, Helseth E. TNF and IL-6 are potent growth factors for OH-2, a novel human myeloma cell line. Eur J Haematol 1994;53:31–7.
7. Filella X, Blade J, Guillermo AL, Molina R, Rozman C, Ballesta AM. Cytokines (IL-6, TNF-α, IL-1α) and soluble interleukin-2 receptor as serum tumor markers in multiple myeloma. Cancer Detect Prev 1996;20:52–6.
8. Lu ZY, Zhang XG, Rodriguez C, et al. Interleukin-10 is a proliferation factor but not a differentiation factor for human myeloma cells. Blood 1995;85:2521–7.
9. Otsuki T, Yata K, Sakaguchi H, et al. IL-10 in myeloma cells. Leuk Lymphoma 2002;43:969–74.
10. Sadat-Sowti B, Debre P, Idziorek T, et al. A lectin-binding soluble factor released by $CD8^+CD57^+$ lymphocytes from AIDS patients inhibits T cell cytotoxicity. Eur J Immunol 1991;21:737–41.
11. Caux C, Massacrier C, Vanbervliet B, Barthelemy C, Liu YJ, Banchereau J. Interleukin 10 inhibits T cell alloreaction induced by human dendritic cells. Int Immunol 1994;6:1177–85.
12. de la Barrera S, Aleman M, Musella R, et al. IL-10 down-regulates costimulatory molecules on *Mycobacterium tuberculosis*-pulsed macrophages and impairs the lytic activity of CD4 and CD8 CTL in tuberculosis patients. Clin Exp Immunol 2004;138: 128–38.
13. Chen L, Linsley PS, Hellstrom KE. Costimulation of T cells for tumor immunity. Immunol Today 1993;14: 483–6.
14. Chen L, McGowan P, Ashe S, et al. Tumor immunogenicity determines the effect of B7 costimulation on T cell-mediated tumor immunity. J Exp Med 1994;179: 523–32.
15. Tamura H, Ogata K, Dong H, Chen L. Immunology of B7-1 and its roles in human diseases. Int J Hematol 2003;78:321–8.
16. Carreno BM, Carter LL, Collins M. Therapeutic opportunities in the B7/CD28 family of ligands and receptors. Curr Opin Pharmacol 2005;5:424–30.
17. Swallow MM, Wallin JJ, Sha WC. B7h, a novel costimulatory homolog of B7.1 and B7.2, is induced by TNFα. Immunity 1999;11:423–32.
18. Hutloff A, Dittrich AM, Beier KC, et al. ICOS is an inducible T-cell co-stimulator structurally and functionally related to CD28. Nature 1999;397:263–6.
19. Wang S, Zhu G, Chapoval AI, et al. Costimulation of T cells by B7-2, a B7-like molecule that binds ICOS. Blood 2000;96:2808–13.
20. Okamoto N, Tezuka K, Kato M, Abe R, Tsuji T. PI3-kinase and MAP-kinase signaling cascades in AILIM/ICOS- and CD28-costimulated T-cells have distinct functions between cell proliferation and IL-10 production. Biochem Biophys Res Commun 2003; 310:691–702.
21. Tamura H, Dan K, Tamada K, et al. Expression of functional B7-2 and B7.2 costimulatory molecules and their prognostic implications in *de novo* acute myeloid leukemia. Clin Cancer Res 2005;11:5708–17.
22. Pope B, Brown RD, Gibson J, Yuen E, Joshua D. B7-2-positive myeloma: incidence, clinical characteristics, prognostic significance, and implications for tumor immunotherapy. Blood 2000;96:1274–9.
23. Ogata K, Satoh C, Tachibana M, et al. Identification and hematopoietic potential of CD45- clonal cells with very immature phenotype ($CD45^-CD34^-$ $CD38^-Lin^-$) in patients with myelodysplastic syndromes. Stem Cells 2005;23:619–30.
24. Durie BG, Salmon SE. A clinical staging system for multiple myeloma. Correlation of measured myeloma cell mass with presenting clinical features, response to treatment, and survival. Cancer 1975;36:842–54.
25. Bataille R, Jégo G, Robillard N, et al. The phenotype of normal, reactive and malignant plasma cells. Identification of "many and multiple myelomas" and of new targets for myeloma therapy. Haematologica 2006;91: 1234–40.
26. Gimeno MJ, Maneiro E, Rendal E, Ramallal M, Sanjurjo L, Blanco FJ. Cell therapy: a therapeutic alternative to treat focal cartilage lesions. Transplant Proc 2005;37:4080–3.
27. Ogata K, Nakamura K, Yokose N, et al. Clinical significance of phenotypic features of blasts in patients with myelodysplastic syndrome. Blood 2002;100: 3887–96.
28. Asosingh K, Vankerkhove V, Van Riet I, Van Camp B, Vanderkerken K. Selective *in vivo* growth of lymphocyte function-associated antigen-1-positive murine myeloma cells. Involvement of function-associated antigen-1-mediated homotypic cell-cell adhesion. Exp Hematol 2003;31:48–55.
29. Schmidmaier R, Morsdorf K, Baumann P, Emmerich B, Meinhardt G. Evidence for cell adhesion-mediated drug resistance of multiple myeloma cells *in vivo*. Int J Biol Markers 2006;21:218–22.
30. Kuchroo VK, Das MP, Brown JA, et al. B7-1 and B7-2 costimulatory molecules activate differentially the Th1/Th2 developmental pathways: application to autoimmune disease therapy. Cell 1995;80:707–18.
31. Wallin JJ, Liang L, Bakardjiev A, Sha WC. Enhancement of $CD8^+$ T cell responses by ICOS/B7h costimulation. J Immunol 2001;167:132–9.
32. Wang G, Zhu L, Hu P, et al. The inhibitory effects of mouse ICOS-Ig gene-modified mouse dendritic cells on T cells. Cell Mol Immunol 2004;1:153–7.
33. Taylor PA, Panoskaltsis-Mortari A, Freeman GJ, et al. Targeting of inducible costimulator (ICOS) expressed on alloreactive T cells down-regulates graft-versus-host disease (GVHD) and facilitates engraftment of allogeneic bone marrow (BM). Blood 2005;105:3372–80.
34. Ansari MJ, Fiorina P, Dada S, et al. Role of ICOS pathway in autoimmune and alloimmune responses in NOD mice. Clin Immunol 2008;126:140–7.
35. Cheever MA, Greenberg PD, Fefer A, Gillis S. Augmentation of the anti-tumor therapeutic efficacy of long-term cultured T lymphocytes by *in vivo* administration of purified interleukin 2. J Exp Med 1982;155: 968–80.
36. Tuttle TM, McCrady CW, Inge TH, Salour M, Bear HD. γ-Interferon plays a key role in T-cell-induced tumor regression. Cancer Res 1993;53:833–9.
37. Maeda A, Yamamoto K, Yamashita K, et al. The expression of co-stimulatory molecules and their relationship to the prognosis of human acute myeloid leukaemia: poor prognosis of B7-2-positive leukaemia. Br J Haematol 1998;102:1257–62.
38. Stremmel C, Greenfield EA, Howard E, Freeman GJ, Kuchroo VK. B7-2 expressed on EL4 lymphoma suppresses antitumor immunity by an interleukin 4-dependent mechanism. J Exp Med 1999;189: 919–30.
39. Thalmeier K, Meissner P, Reisbach G, et al. Constitutive and modulated cytokine expression in two permanent human bone marrow stromal cell lines. Exp Hematol 1996;24:1–10.
40. Silvestris F, Cafforio P, Calvani N, Dammacco F. Impaired osteoblastogenesis in myeloma bone disease: role of upregulated apoptosis by cytokines and malignant plasma cells. Br J Haematol 2004;126:475–86.
41. Ghebeh H, Tulbah A, Mohammed S, et al. Expression of B7-H1 in breast cancer patients is strongly associated with high proliferative Ki-67-expressing tumor cells. Int J Cancer 2007;121:751–8.
42. Teo SK. Properties of thalidomide and its analogues: implications for anticancer therapy. AAPS J 2005;7: E14–9.
43. List AF. Lenalidomide—the phoenix rises. N Engl J Med 2007;357:2183–6.

Cancer Immunol Immunother (2009) 58:1245–1255
DOI 10.1007/s00262-008-0643-x

ORIGINAL ARTICLE

A possible mechanism of intravesical BCG therapy for human bladder carcinoma: involvement of innate effector cells for the inhibition of tumor growth

Tomoe Higuchi · Masumi Shimizu · Atsuko Owaki · Megumi Takahashi · Eiji Shinya · Taiji Nishimura · Hidemi Takahashi

Received: 27 June 2008 / Accepted: 8 December 2008 / Published online: 13 January 2009

Abstract Intravesical bacillus Calmette-Guerin (BCG) therapy is considered the most successful immunotherapy against solid tumors of human bladder carcinoma. To determine the actual effector cells activated by intravesical BCG therapy to inhibit the growth of bladder carcinoma, T24 human bladder tumor cells, expressing very low levels of class I MHC, were co-cultured with allogeneic peripheral blood mononuclear cells (PBMCs) with live BCG. The proliferation of T24 cells was markedly inhibited when BCG-infected dendritic cells (DCs) were added to the culture although the addition of either BCG or uninfected DCs alone did not result in any inhibition. The inhibitory effect was much stronger when the DCs were infected with live BCG rather than with heat-inactivated BCG. The live BCG-infected DCs secreted TNF-α and IL-12 within a day and this secretion continued for at least a week, while the heat-inactivated BCG-infected DCs secreted no IL-12 and little TNF-α. Such secretion of cytokines may activate innate alert cells, and indeed NKT cells expressing IL-12 receptors apparently proliferated and were activated to produce cytocidal perforin among the PBMCs when live BCG-infected DCs were externally added. Moreover, depletion of $\gamma\delta$ T-cells from PBMCs significantly reduced the cytotoxic effect on T24 cells, while depletion of CD8β cells did not affect T24 cell growth. Furthermore, the innate effectors seem to recognize MICA/MICB molecules on T24 via NKG2D receptors. These findings suggest the involvement of innate alert cells activated by the live BCG-infected DCs to inhibit the growth of bladder carcinoma and provide a possible mechanism of intravesical BCG therapy.

Keywords Bladder cancer · Dendritic cells · Innate immunity · BCG · NKT cells

T. Higuchi · M. Shimizu · A. Owaki · M. Takahashi · E. Shinya · H. Takahashi (✉)
Department of Microbiology and Immunology, Nippon Medical School, 1-1-5 Sendagi, Bunkyo-ku, Tokyo 113-8602, Japan
e-mail: htkuhkai@nms.ac.jp

T. Higuchi · T. Nishimura
Department of Urology, Nippon Medical School, Tokyo 113-8602, Japan

Introduction

Intravesical bacillus Calmette-Guerin (BCG) therapy is considered the most successful immunotherapy against solid tumors in cases of human superficial bladder carcinoma particularly in preventing from its recurrence [1, 4]. Intravesical immunotherapy with live BCG results in a massive local immune response characterized by the secretion of various cytokines in the urine [14, 27] or bladder tissue as well as by the infiltration of granulocytes and mononuclear cells into the bladder wall after repeated treatment with BCG instillation [3, 21], indicating the immunopathological responses induced at the local mucosal compartment may correlate with the BCG-mediated antitumor effect. However, neither the precise mechanisms nor the actual effector cells underlying the anti-tumor effect that BCG therapy stimulates remain to be elucidated.

The bladder is a confined mucosal compartment, where BCG is able to be maintained at a high concentration and thus may achieve long-lasting, continuous immune activation, which seems to better stimulate innate local immunity having broad cross-reactivity with less memory rather than acquired systemic immunity with high specificity and memory originated from rearranged genes. Therefore, live

BCG appears to activate various types of innate immune effectors such as γδT lymphocytes [17, 18] and CD1 molecule-restricted lipid/glycolipid antigen-specific T cells including CD1d-restricted natural killer T (NKT) cells [12, 13] via live BCG-infected dendritic cells (DCs). Such DCs express not only peptide antigen-loaded individually restricted class I and II MHC molecules but also species-specific CD1 molecules on their surface to present BCG-derived lipid/glycolipid antigens [15, 20]. Indeed, findings that live BCG-infected DCs can be recognized by CD1 molecule-restricted but not by class I MHC molecule-restricted $CD8^+$ T cells [16] and that the Vγ2Vδ2 T lymphocytes response to BCG by immunization in macaques with live BCG [5] have recently been reported. Moreover, a close relationship between BCG-immunization, and NKT cell activation has also been shown [9]. Therefore, continuous stimulation in the confined bladder space with live BCG may activate those local innate effectors, which may control bladder cancer expansion in vivo.

The cell line T24, a well-known cell for human bladder cancer [19], expresses markedly down-modulated MHC class I molecules on the cell surface in comparison with normal peripheral blood mononuclear cells (PBMCs). Hence, the T24 line is possibly regulated by cells in a class I MHC molecule-unrelated manner rather than by the autologous class I MHC molecule-restricted conventional CD8-positive cytotoxic T lymphocytes (CTLs). Therefore, we co-cultured T24 cells with allogeneic PBMCs pretreated with live BCG to determine the actual cells activated by the BCG for controlling T24 tumor cell proliferation and elimination, and found that innate alert cells such as Vγ2Vδ2 T cells and particularly NKT cells derived from allogeneic PBMCs activated by the live BCG-pretreated DCs appear to inhibit the proliferation of T24 tumor cells as well as eliminate them. The findings shown in the present study strongly suggest the involvement of innate alert effectors in controlling bladder cancer growth and shed light on the actual feature of the mechanisms for the anti-tumor effect of intravesical BCG therapy.

Materials and methods

Cell lines

Human urinary bladder carcinoma T24 cells (ATCC HTB-4) were cultured in McCoy's 5a medium (Invitrogen, Carlsbad, CA) supplemented with 10% FCS (HyClone Laboratories, Logan, UT), 50 U/ml penicillin (Invitrogen), and 50 mg/ml streptomycin (Invitrogen). Human colon cancer derived HCT116 cells (ATCC CCL 247), C1R cells were cultured in Dulbecco's modified Eagle's medium (Sigma-Aldrich, St Louis, MO) supplemented with 10% FCS (HyClone), 50 U/ml penicillin, and 50 mg/ml streptomycin (Invitrogen). Myelogenous leukemia K562 cells, and T lymphoblast Jurkat cells were cultured in RPMI 1640 (Sigma-Aldrich, St Louis, MO)-based complete T-cell medium (CTM) [25] supplemented with 10% FCS, 2 mM L-glutamine (ICN Biomedicals, Aurora, OH), 100 units/ml penicillin, 100 μg/ml streptomycin, 1 mM HEPES (Invitrogen), 1 mM sodium pyruvate (Invitrogen), 50 mM 2-mercaptoethanol (2-ME) (Invitrogen).

Infection of DCs with live or heat-inactivated BCG

A lyophilized preparation of BCG, the Tokyo 172 strain (12 mg dry weight per ample) (Japan BCG Laboratory, Tokyo, Japan) was used to carry out the experiments. For the infection experiments, BCG was harvested at a mid-log growth phase, washed, and suspended in RPMI 1640 medium supplemented with 10% FCS. The suspension was passed through a 5-μm pore size filter to obtain single-cell bacteria. The viability of bacteria was constantly >90%. The BCG preparation was divided into two equal aliquots; one incubated for 30 min at 85°C to kill the bacteria and the other left at room temperature as reported recently [16].

Generation of DCs from PBMCs and their treatment with BCG

DCs were obtained from PBMCs as described recently [26]. In brief, PBMCs were freshly isolated with Ficoll-Hypaque (Amersham-Pharmacia Biotech, Uppsala, Sweden) from peripheral blood of healthy volunteers, and $CD14^+$ monocytes were immediately separated by magnetic depletion using a monocyte isolation kit (Miltenyi Biotec, Bergisch Gladbach, Germany) containing hapten-conjugated antibodies to CD3, CD7, CD19, CD45RA, CD56, and anti-IgE Abs and a magnetic cell separator (MACS, Miltenyi Biotec) according to the manufacturer's instructions, routinely resulting in >90% purity of $CD14^+$ cells. Cells were cultured in 24-well plates for 6–7 days in CTM supplemented with 200 ng/ml GM-CSF (PeproTech, Rocky Hill, NJ), and 10 ng/ml IL-4 (Biosource Intl., Camarillo, CA) to obtain DCs. For the treatment with BCG, 1×10^5 DCs in 1 ml of CTM were incubated overnight with 0.1 mg of either live BCG or heat-inactivated BCG. After being washed three times with RPMI1640 medium, the BCG-treated DCs were further co-cultured with 1×10^6 PBMCs of the same donor to carry out the experiments.

Antibodies and flow-cytometric analysis

Fluorescein isothiocyanate (FITC)-conjugated anti-human monoclonal antibodies (mAbs) to mouse IgG1κ, isotype control (MOP-21), HLA-ABC (G46-2.6), CD3 (H1T3a),

CD161 (DX12), CD80 (B7-1) (L307.4), CD86 (B70/B7-2) [2331(FUN-1)], as well as phycoerythrin (PE)-conjugated mouse IgG1κ, isotype control, CD3, CD56 (B159), and unlabeled anti-human CD3, CD4 (RPA-T4), Vδ2 (B6), and CD161, were all purchased from BD Biosciences (San Diego, CA). Unlabeled anti-human CD8β (2ST8.5H7) mAb was purchased from IMMUNOTECH (Marseille, Cedex, France). Cells were stained with the relevant antibody on ice for 30 min in phosphate-buffered saline (PBS) with 2% FCS and 0.01 M sodium azide (PBS-based medium), washed twice, and re-suspended in the PBS-based medium. Then, the labeled cells were analyzed with a FACScan (BD Biosciences) using CellQuest software (BD Biosciences). Live cells were gated based on propidium iodide gating.

Depletion of cells from PBMCs

To deplete Vδ2-positive cells, PBMCs were incubated with mouse anti-human Vδ2 mAb (B6) for 30 min at 4°C and washed three times to remove free mAb. Then the stained cells were further incubated with magnetic beads-conjugated anti-mouse IgG (Dynabeads Pan Mouse IgG) (DYNAL BIOTECH, Oslo, Norway), and Vδ2-positive cells were eliminated by magnetic device (Perspective Biosystems, Framingham, MA) following the manufacturer's instruction. CD8β, CD3, CD161, and CD4-positive cells were also depleted using the same procedure.

Quantification of cytokine production from BCG-treated DCs by ELISA

Monocyte-derived DCs (1×10^6) were incubated with 1 ml of CTM containing 0.1 mg of BCG in 24-well culture plate for 2–3 days and the culture supernatants were collected and stored at −80°C until the measurement of cytokines. Production of TNF-α, IL-12, IL-10, and IL-4 was measured using the DuoSet ELISA Development Kit (R&D systems, Minneapolis, MN) according to the manufacturer's instructions.

Chromium-51 release assay

The cytotoxicity of BCG-activated cells was measured by a standard 4-h ^{51}Cr-release assay using T-24 human bladder cancer cells or NK-sensitive K562 myelogenous leukemia cells as targets. In brief, various numbers of effector cells were incubated with 3×10^3 ^{51}Cr-labeled targets for 4 h at 37°C in 200 µl of RPMI 1640 medium containing 10% FCS in round-bottomed 96-well cell culture plates (BD Biosciences). After incubation, the plates were centrifuged for 10 min at 330×*g*, and 100 µl of cell-free supernatant was collected to measure radioactivity with a Packard Auto-Gamma 5650 counter (Hewlett-Packard Japan, Tokyo, Japan). Maximum release was determined from the supernatant of cells that had been lysed by the addition of 5% Triton ×-100 and spontaneous release was determined from target cells incubated without added effector cells. The percent specific lysis was calculated as 100× (experimental release − spontaneous release)/(maximum release − spontaneous release). Standard errors of the means of triplicate cultures were always <5% of the mean. Data are expressed as the mean ± SEM. Each experiment was performed at least three times.

T24 growth inhibition assay

The T24 growth inhibition assay was performed by incubating 1×10^4 T24 cells with 5×10^4 or 1×10^5 freshly isolated allogeneic PBMCs in 200 µl of CTM for 3 days at 37°C in 5% CO_2 based on a recent study [22]. Samples were cultured in triplicate on 96-well U-bottom plates. The cells were then labeled for 16 h with 1 µCi/well of tritiated thymidine (^{3}H-TdR; MP Biomedicals, Morgan, CA), harvested in an automated plate harvester (TomTech, Orange, CT), and counted in a 1,450 Micro Beta TRILUX scintillation spectrometer (Wallac, Gaithersburg, MD). Data are expressed as the mean count per minute (cpm) ± SEM.

RT-PCR for CD1d mRNA in T24 cells

Total RNA was extracted from T24, Jurkat, and HCT cells using the RNeasy Protocol Mini Kit (Qiagen, Valencia, CA) according to the manufacturer's instructions. RNA (2 µg) was reverse transcribed with oligo-(dT)18 (Perkin Elmer, Wellesley) priming and Superscript III (Invitrogen) reverse transcriptase in a 20 µg reaction mixture at 50°C for 60 min. A measure of 1 µl (equal to about 200 ng) of the cDNA product was then subjected to 30 cycles of 30 s at 94°C, 1 min at 64°C, and 1 min final extension at 72°C, with a thermocycler (PCR express; Hybaid, Teddington, Middlesex, UK). The amplification was performed in a reaction volume of 20 µl with LA PCR buffer (Takara, Shiga, Japan), composed of 2.5 mM $MgCl_2$, 0.3 nM of each deoxynucleotide triphosphate, 2.5 mM of each primer, and 1 U of LA Taq polymerase (Takara). The following oligonucleotide primers were designed from the published cDNA sequence [6]: GAPDH sense-primer (5′-GCCTCAA GATCATCAGCAATGC-3′) and antisense-primer (5′-AT GCCAGTGAGCTTCCCGTTC-3′), human CD1d (hCD1d) full-length sense-primer (5′-CGGGATCCATGGGGTGC CTGCTGTTTCTG-3′), antisense-primer (5′-ATTTGCGG CCGCCAGGACGCCCTGAT-3′), hCD1d short fragment sense-primer (5′-CTCCAGATCTCGTCCTTCGCCATT-3′), antisense-primer (5′-TTGAATGGCCAAGTTTACCCAA AG-3′).

Measurement of cytotoxicity by BCG-activated innate effctors through NKG2D-receptor against MICA/MICB molecules on T24 tumor cells

Cytotoxicity of innate effectors activated by live BCG-treated DC against T24 cells was investigated using 51-chromium release assay shown above in the presence of various blocking antibodies such as anti-human MICA/MICB (6D4) (BioLegend, San Diego, CA), anti-human NKG2D (CD314)-specific mouse mAbs (1D11) (BioLegend), or isotype-matched control mouse IgG1κ (BD Biosciences). $CD3^+CD56^+$ NKT cells were sorted out with FACS-Vantage SE (BD Biosciences) according to the manufacturer's instruction.

Results

T24 growth inhibition by allogeneic PBMCs activated with live BCG-treated DCs

The bladder cancer cell line T24, a well-known cell for human bladder cancer, expresses markedly reduced levels of MHC class I molecules on the cell surface in comparison with normal PBMCs (data not shown). Thus, the T24 line is possibly regulated by cells in a class I MHC molecule-unrelated manner rather than by the autologous class I MHC molecule-restricted conventional CTLs. Therefore, we used allogeneic PBMCs to gain insight into the actual cells activated by BCG for controlling T24 tumor cell proliferation and elimination.

When 5×10^4 or 1×10^5 freshly isolated allogeneic PBMCs were co-cultured with 1×10^4 T24 cells in the presence of live BCG, strong inhibition of T24 cell proliferation measured with ^{3}H-TdR was observed as compared with BCG-absent control (Fig. 1a). Because the BCG-susceptible cells are thought to be DCs, DCs from the PBMCs were pretreated with (0.1 mg/ml) live BCG for 6 h at 37°C. Then, after confirmation that the addition of live BCG-pretreated DCs alone did not affect the T24 cell proliferation, 1×10^4 T24 cells were incubated with an equal number of the indicated DCs together with 5×10^4 or 1×10^5 allogeneic PBMCs of the same donor. Profound inhibition of T24 cell proliferation was observed when live BCG-infected DCs were co-cultured with PBMCs of the same donor (Fig. 1b). Moreover, the effect of live or heat-inactivated BCG-treated DCs on T24 cell proliferation was also examined. As indicated in Fig. 1c, the addition of heat-inactivated BCG-pretreated DCs resulted in partial inhibition of the proliferation. These results indicated that some cells derived from allogeneic PBMCs activated by the live BCG-pretreated DCs might gain the capacity to inhibit the proliferation of T24 tumor cells.

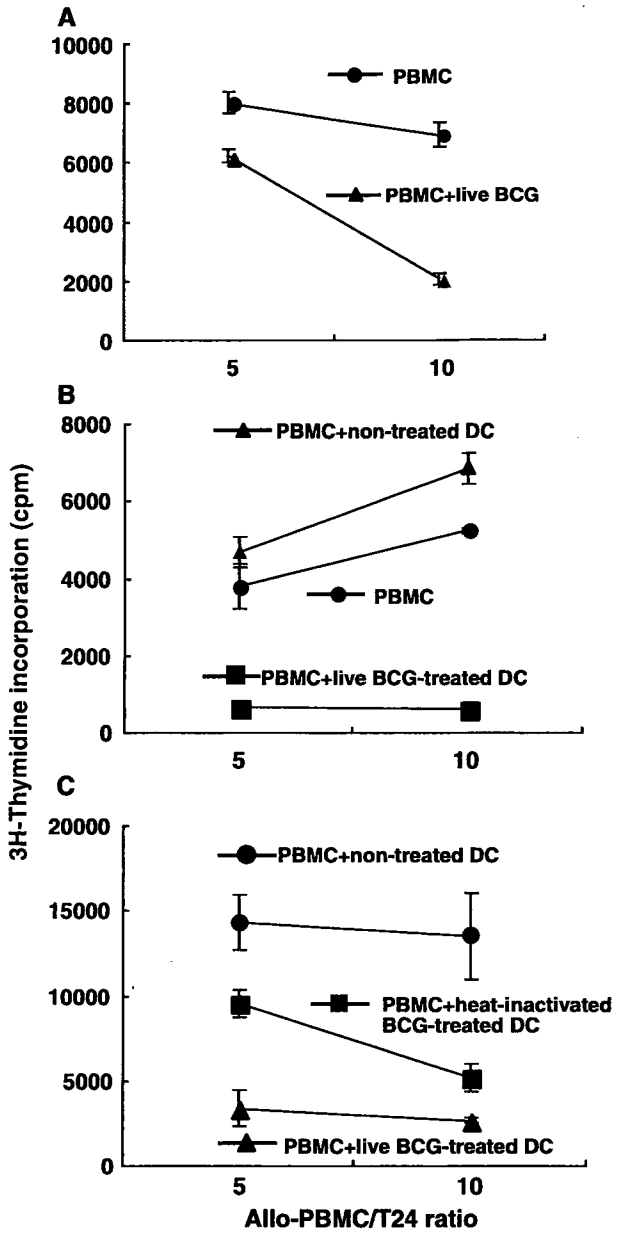

Fig. 1 Inhibition of T24 growth by allogeneic PBMCs activated with live BCG-treated DCs. **a** When 5×10^4 or 1×10^5 freshly isolated allogeneic PBMCs were co-cultured with 1×10^4 T24 cells in the presence of live BCG (*closed triangle*), strong inhibition of T24 cell proliferation measured by ^{3}H-TdR was observed in comparison with the BCG-absent control (*closed circle*). **b** T24 cells (1×10^4) were incubated with 5×10^4 or 1×10^5 allogeneic PBMCs. Profound inhibition of T24 cell proliferation was observed when live BCG-infected DCs were co-cultured with PBMCs (*closed square*). However, no inhibition was observed when T24 cells were co-cultured either with PBMC alone (*closed circle*) or with PBMC plus BCG-uninfected DCs (*closed triangle*). **c** T24 cells (1×10^4) were incubated with 5×10^4 or 1×10^5 allogeneic PBMCs plus live BCG-treated DCs (*closed triangle*), heat-inactivated BCG-treated DCs (*closed square*), or control untreated DCs (*closed circle*). Again, strong inhibition of T24 cell proliferation was observed when PBMCs were co-cultured with live BCG-infected DCs (*closed triangle*) and partial inhibition was seen when they were co-cultured with heat-inactivated BCG-treated DCs (*closed square*)

Kinetics of cytokine secretion by live BCG-treated DCs

Next, the live BCG-treated DCs were compared with the inactivated BCG-treated DCs in terms of the kinetics of cytokine secretion. As demonstrated in Fig. 2a with closed columns, live BCG-treated DCs secreted quite a large amount of IL-12 2–3 days after the incubation, however, heat-inactivated BCG-treated DCs shown with open columns secreted almost no detectable amount of IL-12. As for TNF-α, live BCG-treated DCs secreted more of it than heat-inactivated BCG-treated DCs (Fig. 2b). In contrast, the amount of IL-10 secretion was almost the same between the two (Fig. 2c). Furthermore, the expression levels of co-stimulated molecules, CD80 and CD86, were higher in live BCG-treated DCs (data not shown).

T24 growth inhibition was mainly mediated through CD8β-negative T cells

These findings suggest live BCG-activated DCs to activate effectors from PBMCs to inhibit T24 cell proliferation through the secretion of IL-12 and TNF-α. Therefore, to examine the actual cells that eliminate T24, CD3-positive T cells were eliminated from among the activated PBMCs with live BCG-treated DCs, and the cytotoxicity against ^{51}Cr-labeled T24 targets was measured. The cytotoxicity was significantly reduced by the elimination of the CD3-positive cells (Fig. 3a). The remaining weak cytotoxicity, shown as open circles in Fig. 3a, might be due to the effect of activated non-T cells such as NK cells. Moreover, the cytotoxicity against T24 cells was not inhibited by the elimination of CD8β-positive cells (shown as closed squares) (Fig. 3b). These results suggest that the class I MHC molecule-restricted conventional CD8β-positive CTL do not seem to be involved in this T24-related cytotoxicity.

T24 tumor growth was partially inhibited by Vγ2Vδ2 T cells

Collectively, the cytotoxity against T24 cells mediated through live BCG-treated DCs appeared to be provided by the major effectors of innate immunity; NK cells, NKT cells, and γδ T cells. Thus, we then examined the possible involvement of γδT cell effectors in the elimination of tumor cells. γδ T cells are classified into two distinct types, type-1 expressing Vγ1Vδ1 T-cell receptor (TCR) and type-2 expressing Vγ2Vδ2 TCR, with the majority of cells generated by BCG reported to be the latter type-2 γδ T cells [11]. When the Vδ2-positive type-2 γδT cells were eliminated from live BCG-activated PBMCs, slight inhibition of the cytotoxicity against T24 cells was observed and this was apparent when the Vδ2-positive cells were depleted from PBMCs before co-culturing with BCG-treated DCs

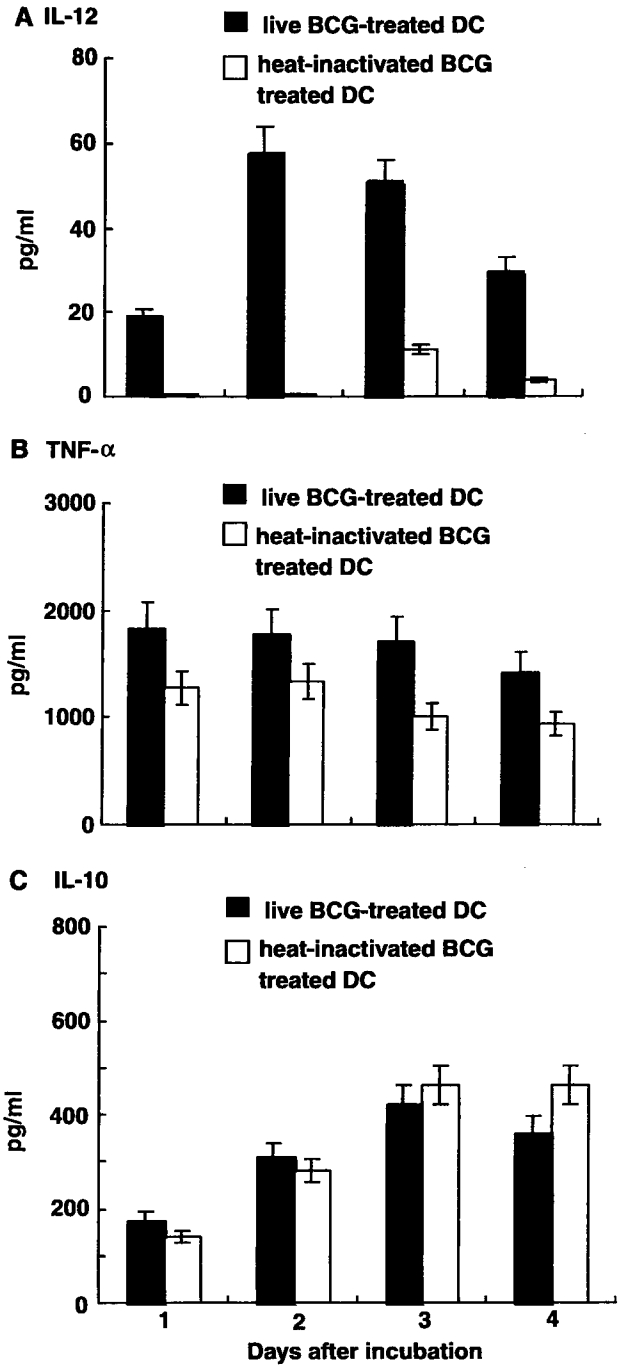

Fig. 2 Measurement of cytokine production by BCG-treated DCs.The difference in the kinetics of cytokine secretion between live BCG-treated DCs and inactivated BCG-treated DCs was compared. Live BCG-treated DCs (*closed column*) secreted predominantly large amounts of IL-12 (**a**) and larger amounts of TNF-α (**b**) than heat-inactivated BCG-treated DCs (*open column*), while the amount of IL-10 secretion (**c**) was lower than in the case of heat-inactivated BCG-treated DCs

(Fig. 3c). Moreover, PBMCs treated with risedronate, an activator of Vδ2 [8], showed strong anti-tumor effect against T24 cells (Fig. 3d). These results indicate the involvement of live BCG-activated Vγ2Vδ2 TCR-expressing type-2 γδT cells in the elimination of T24 tumor cells.

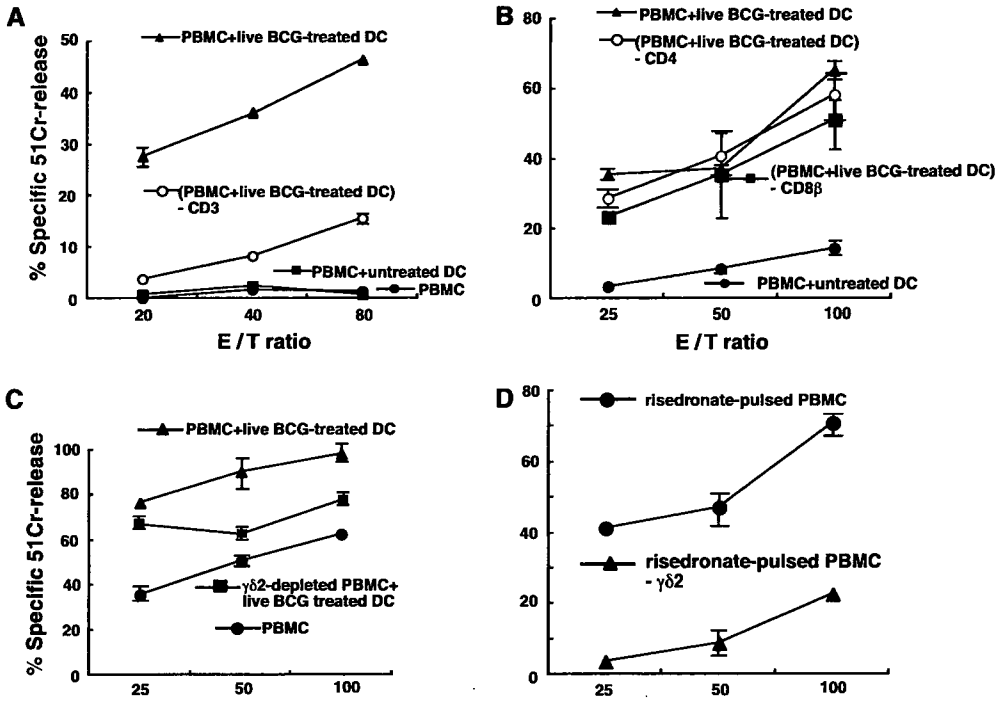

Fig. 3 T24 growth inhibition was partially mediated through CD8β-negative Vγ2Vδ2 T cells. **a** When CD3-positive T cells were eliminated from among the activated PBMCs with live BCG-treated DCs, the cytotoxicity against T24 tumor cells was significantly reduced (*open circle*) almost to the basal level mediated by normal PBMC (*closed circle*) or PBMC plus untreated DCs (*closed square*) in comparison with positive PBMCs activated with live BCG-treated DCs (*closed triangle*) and the remaining weak cytotoxicity might be due to the effect of activated non-T cells such as NK cells. **b** Such cytotoxicity against T24 cells was not abrogated by the elimination of CD8β-positive cells (*closed square*). The results suggest the class I MHC molecule-restricted conventional CD8β-positive CTLs do not seem to be involved in this T24-related cytotoxicity. The elimination of CD4-positive cells (*open circle*) from live BCG-activated PBMCs (*closed triangle*) did not result in any reduction of cytotoxicity against T24 targets in comparison with the basal level mediated by normal PBMC plus untreated DCs (*closed circle*). **c** When the Vδ2-positive cells were depleted from PBMCs before co-culturing with live BCG-treated DCs (*closed square*), the cytotoxicity against T24 was apparently reduced nearly by half in comparison with PBMCs activated with live BCG-treated DCs (*closed triangle*). **d** Moreover, the Vδ2 cell-enriched population from PBMCs co-cultured with risedronate showed a strong anti-tumor effect against T24 cells (*closed circle*). The elimination of type-2 $\gamma\delta$T cells resulted in a significant reduction in the cytotoxicity against T24 cells (*closed triangle*). These results indicate the involvement of live BCG-activated Vγ2Vδ2 TCR-expressing type-2 $\gamma\delta$T cells in the elimination of T24 tumor cells

Effect of depletion of CD161-positive cells on T24 growth

CD161 is known as a marker for NK and NKT cells. Thus, to examine the effect of NK and NKT cells on the elimination of T24 cells, CD161-positive cells were depleted from PBMCs activated by live BCG-treated DCs, and their elimination was confirmed by flowcytometry (Fig. 4a). After confirming that the CD161-positive cells were depleted, the cytotoxicity of the remaining cells against T24 cell was measured by ^{51}Cr-release assay. A profound reduction in the cytotoxity was observed when the CD161-positive cells were eliminated and the reduced cytotoxicity was slightly greater than that of the activated PBMCs co-cultured with live BCG-treated DCs (Fig. 4b). These findings suggest the residual $\gamma\delta$T cells after the elimination of CD161-positive cells to be slightly more cytotoxic than the activated NK cells in PBMCs. Also, as shown in Fig. 4c, that the live BCG-activated PBMCs showed far stronger cytotoxicity than untreated PBMCs against K562 cells that are known to be sensitive to NK cells indicates NK cells to be less cytotoxic to T24 tumor cells than innate $\gamma\delta$T or NKT cells. Taken together, these results suggest the most potent effectors among the live BCG-activated cells against T24 seem to be NKT cells.

Significant production and increase of perforin in the NKT cell population among PBMCs co-cultured with live BCG-treated DCs

Thus, to confirm the actual number and increase of NKT cells among PBMCs co-cultured with live BCG-treated DCs, a flow-cytometric analysis was performed. The results showed that the number of both $CD3^+CD56^+$ cells and $CD3^+CD161^+$ NKT cells but not $CD3^-CD56^+$ or $CD3^-CD161^+$ NK cells apparently increased among those PBMCs activated by live BCG-treated DCs but not by heat-

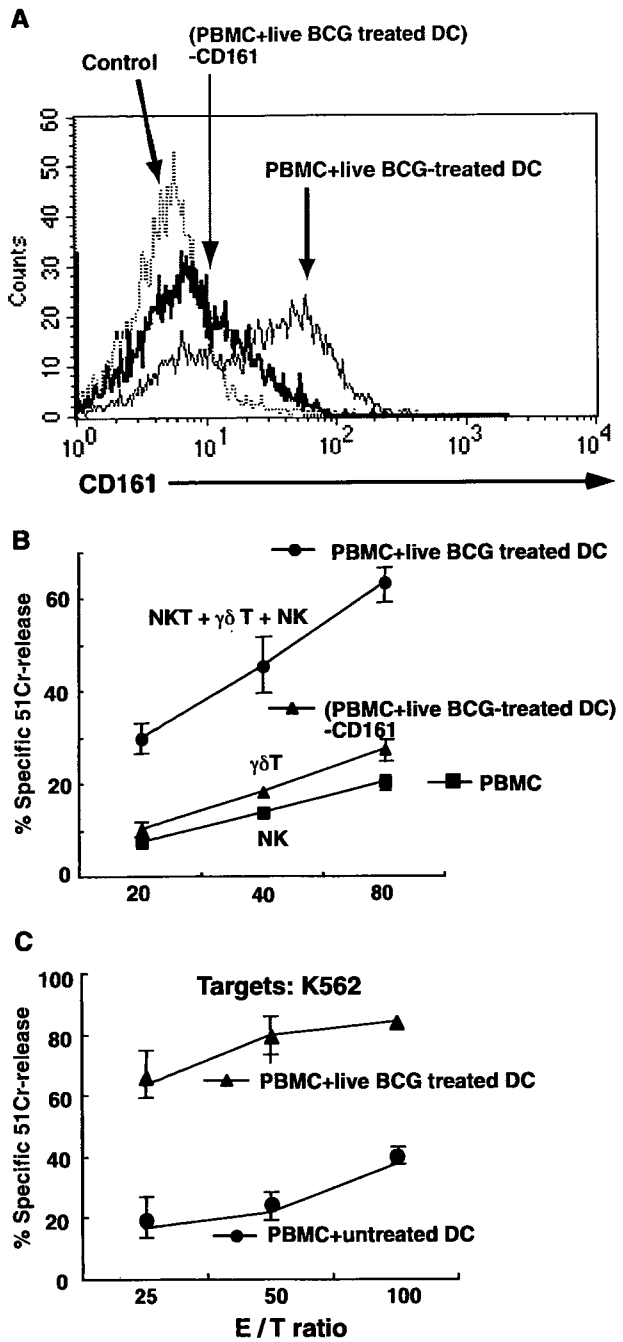

Fig. 4 Effect of CD161 positive cells depletion on T24 growth. **a** The elimination of CD161-positive cells was confirmed by flow cytometry. **b** The remaining cells after the elimination of CD161-positive cells (*closed triangle*) showed a profound reduction of cytotoxicity against T24 cells compared to live BCG-activated PBMCs (*closed circle*). The findings suggest that the residual γδT cells after the elimination of CD161-positive cells had slightly stronger cytotoxicity than the activated NK cells in PBMCs (*closed square*). **c** PBMCs activated by live BCG-treated DCs (*closed triangle*) showed far stronger cytotoxicity than BCG-untreated PBMCs (*closed circle*) against NK-sensitive K562 cells. These results indicate that NK cells have weaker cytotoxicity against T24 tumor cells than innate γδT or NKT cells activated by live BCG-treated DCs

inactivated BCG-treated DCs (Fig. 5a). Therefore, the number of NKT cells certainly increased in the live BCG-activated population. Moreover, those live BCG-activated NKT cells actually produced to secrete cytocidal molecules like perforin (Fig. 5b) or granzyme B (data not shown). Also, it should be noted that the live BCG-activated γδT cells became effector/memory state expressing CD45RO from naïve state expressing CD45RA although the number of γδT cells did not altered (data not shown).

Increased NKT cells inhibited T24 cells in a CD1d-unrestricted fashion

In general, NKT cells recognize glycolipid antigens presented by CD1d [23]. To clarify whether the live BCG-activated NKT cells see T24 tumor antigens in a CD1d-restricted manner, the expression of CD1d on T24 cells was investigated. Despite careful and intense examination, neither mRNA encoding CD1d nor the surface expression of CD1d was detected in not only untreated T24 cells but also BCG-treated ones (Fig. 6a, b), indicating that T24 will not express CD1d molecules even incorporating BCG into their cellular component.

Therefore, to exclude the possibility of subtle expression for functional CD1d on T24 cells after the BCG treatment, an established human NKT line (HT-AC2) that recognizes α-galactosyl ceramide (α-GalCer) and secretes IL-4 in a CD1d-restricted manner (Shimizu & Takahashi, manuscript in preparation) and C1R/CD1d cells expressing human CD1d gene, we examined whether NKT cells can recognize T24 cells in the presence of α-GalCer. No IL-4 was detected in the supernatant of the NKT cell line co-cultured with α-GalCer-pulsed T24 as well as BCG-treated T24 cells (Fig. 6c). Collectively, NKT cells but not NK cells induced by the live BCG-activated DCs seem to predominantly eliminate or suppress T24 tumor cells in a CD1d-unrestricted, α-GalCer independent fashion.

Possible tumor cell ligands for BCG-activated NKT cell recognition

Because NKG2D expression was observed on the NKT cells or γδT cells expanded from live BCG-treated PBMCs (data not shown), blocking effect of antibodies for stress-associated tumor cell-specific molecules such as MICA/MICB [2, 10], the counterparts of NKG2D receptor, on the recognition of T24 cells was examined based on the recent finding [28]. As demonstrated in Fig. 7a, significant inhibition of the cytotoxicity mediated by activated NKT cells was seen when anti-MICA/MICB specific antibody was added, although isotype-

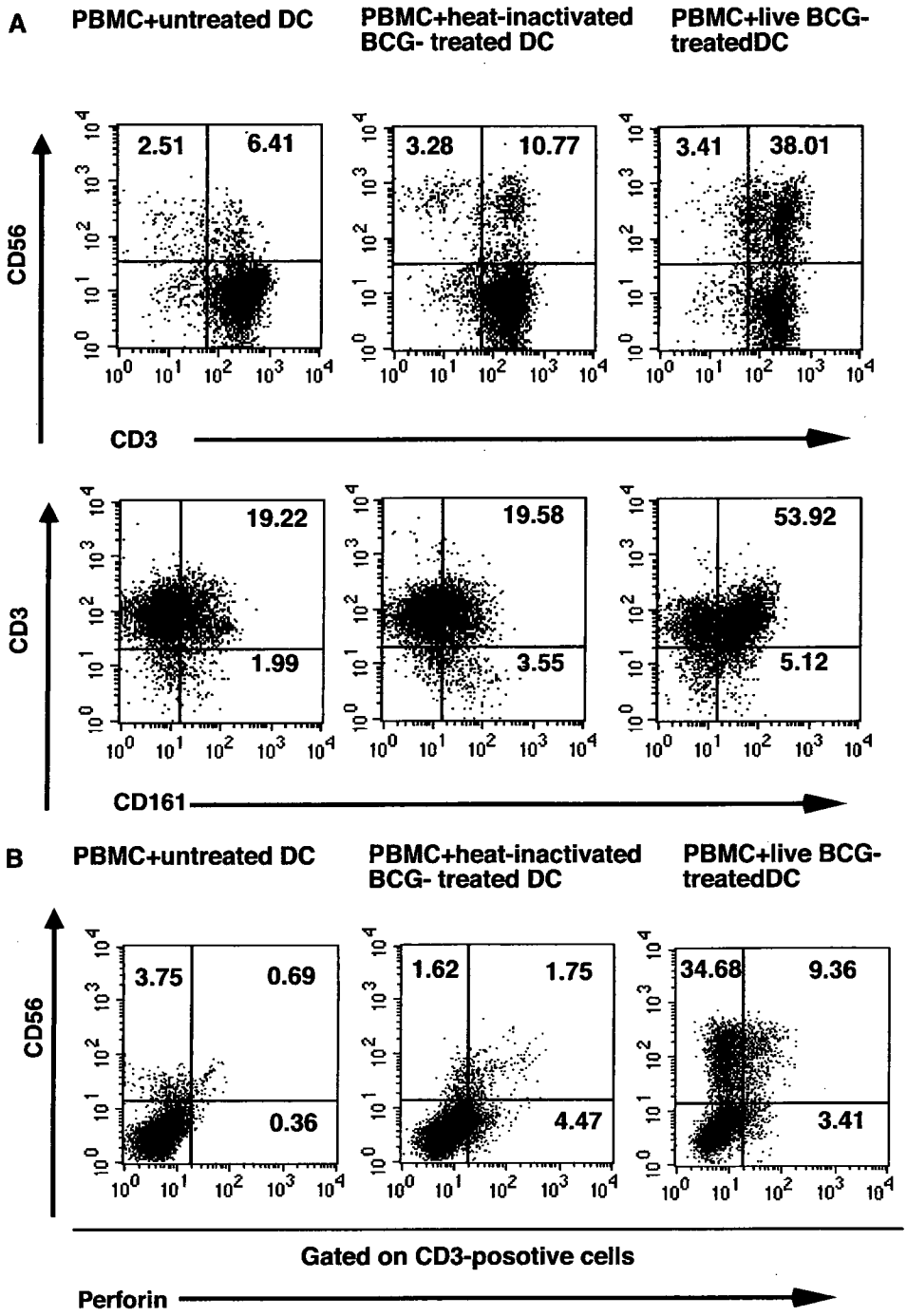

Fig. 5 Significant increase and perforin production in the number of NKT cells among PBMCs activated by live BCG-treated DCs. **a** Flow-cytometric analysis showed that the number of both $CD3^+CD56^+$ cells, and $CD3^+CD161^+$ NKT cells but not $CD3^-CD56^+$ or $CD3^-CD161^+$ NK cells apparently increased among those PBMCs activated by live BCG-treated DCs but not by heat-inactivated BCG-treated DCs. Therefore, the number of NKT cells certainly increased in the live BCG-activated population. **b** The live BCG-activated NKT cells actually produced to secrete cytocidal molecules like perforin, while heat-inactivated BCG-associated NKT did not

matched antibody did not show any inhibition for their cytotoxicity. Moderate inhibition was also seen when the NKG2D receptors blocked by their specific antibody (Fig. 7a). Similarly, cytotoxicity against T24 cells by live BCG-treated PBMCs containing mostly activated NKT cells as well as some $\gamma\delta$T and NK cells was markedly inhibited by anti-MICA/MICB specific antibody (Fig. 7b). Therefore, MICA/MICB molecules on the T24 cells appear to be a possible tumor cell ligands for BCG-activated innate NKT cell recognition.

Discussion

Intravesical BCG therapy is probably the most effective immunotherapy for recurrent superficial bladder cancer. As far as we have examined, the anti-tumor effect does not appear to be due to direct cytotoxicity of BCG itself. In fact, it was recently reported that the treatment of the urothelial carcinoma cell line T24 with BCG did not induce apoptosis, and BCG inhibited camptothecin-mediated apoptosis [7]. Similarly, treatment of T24 cells with BCG

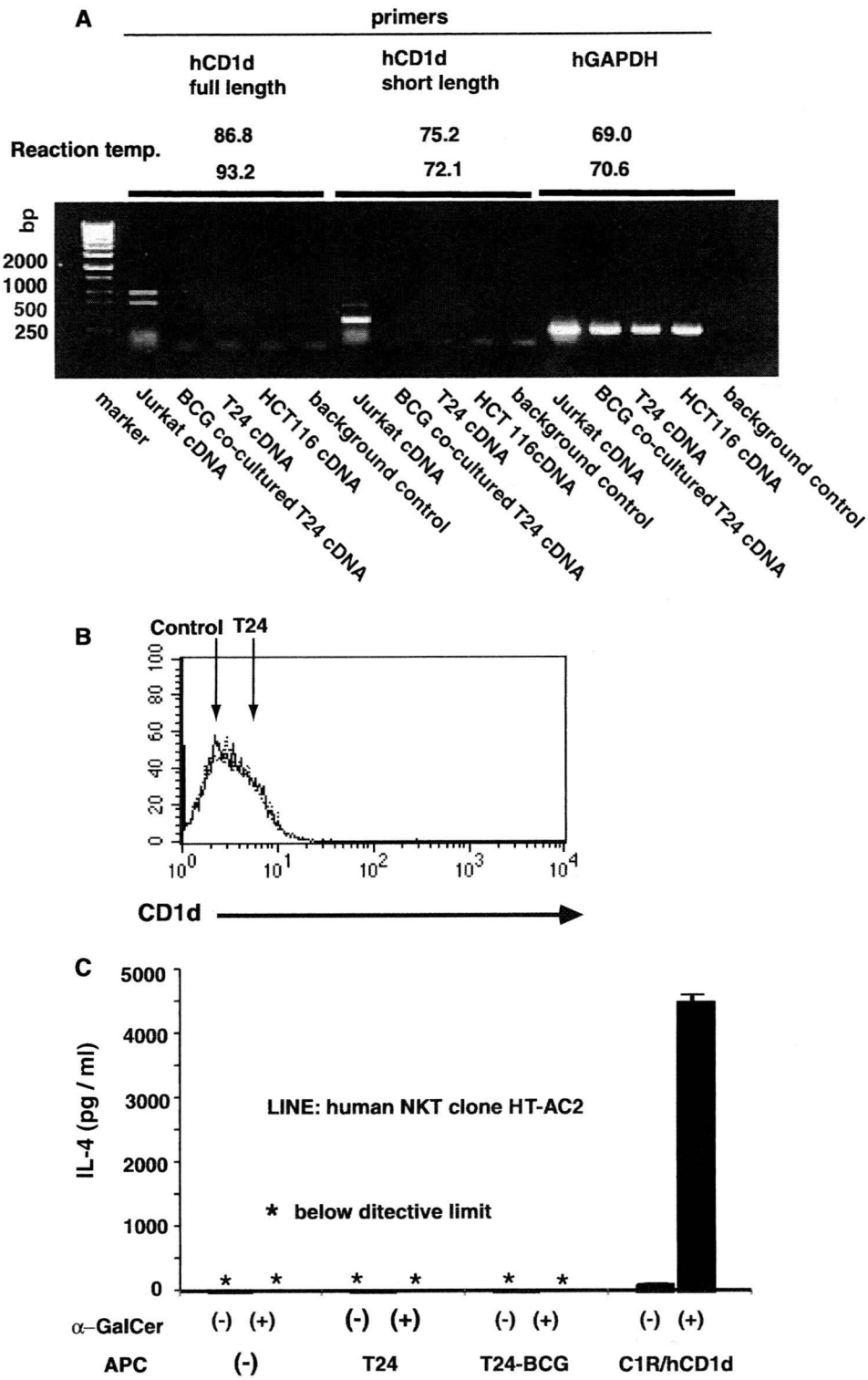

Fig. 6 Inhibition of T24 tumor growth by the BCG-activated NKT cells was mediated in a CD1d-unrestricted manner. NKT cells are usually recognized as antigens in association with CD1d molecules. Thus, **a** both internal mRNA for CD1d expression and **b** external surface expression were examined in T24 tumor cells. However, CD1d expression could not be detected at all even after co-cultured with live BCG. **c** Therefore, using an established human NKT line (HT-AC2) that recognizes α-galactosyl ceramide (α-GalCer) in a CD1d-restricted manner and secretes IL-4 (Shimizu & Takahashi, manuscript in preparation) and CD1d-expressing C1R cells (C1R/hCD1d), we investigated whether NKT cells can recognize live BCG-treated (T24-BCG) or untretaed T24 cells in the presence of α-GalCer. No IL-4 was detected in the supernatant of NKT cells co-cultured with α-GalCer-pulsed those T24 cells. Taken together, NKT cells generated by the live BCG-activated DCs seem to inhibit T24 tumor cell growth in a CD1d-unrestricted manner

did not cause any apoptotic changes as examined with a TUNEL assay [24]. Therefore, BCG itself does not eliminate T24 tumor cells but rather some immune system activated by BCG may indirectly inhibit the growth of these cells or eliminate them.

The body has two distinct immune systems to suppress tumor growth or eliminate tumor cells. One is systemic acquired immunity with highly specific effectors such as class I MHC molecule-restricted $CD8^+$ CTLs, class II MHC molecule-restricted $CD4^+$ T cells, and specific antibodies. These effectors express specific receptors originating from rearranged genes established by periodic stimulation. The magnitude of specific responses will increase synergistically with the number of stimulations.

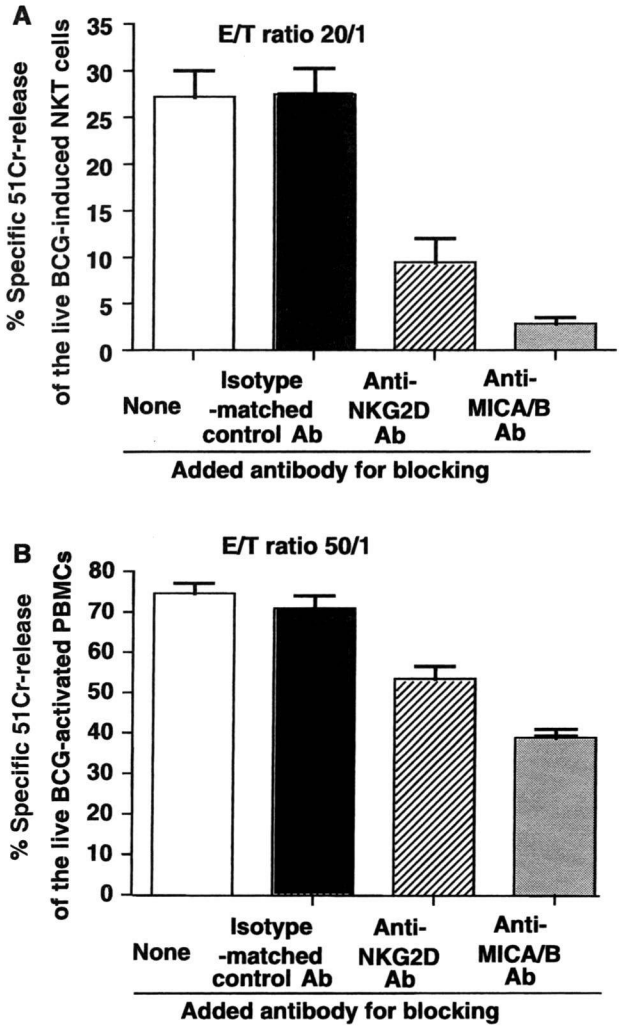

Fig. 7 Possible tumor cell ligands for BCG-activated NKT cell recognition. **a** Effect of antibodies for blocking stress-associated tumor cell-specific molecules such as MICA/MICB, the counterparts of NKG2D receptor, on the recognition of T24 cells was examined. Significant inhibition of the cytotoxicity mediated by activated NKT cells was seen when anti-MICA/MICB specific antibody was added, although isotype-matched antibody did not show any inhibition for their cytotoxicity. Moderate inhibition was also seen when the NKG2D receptors blocked by their specific antibody. **b** Cytotoxicity against T24 cells by live BCG-treated PBMCs containing mostly activated NKT cells as well as some $\gamma\delta$T cells and NK cells was also markedly inhibited by anti-MICA/MICB specific antibody

In contrast, local innate immunity involves toll-like receptors (TLR), $\gamma\delta$ TCR, or invariant NKT–TCR having diverse cross-reactivity without requiring the strict gene-rearrangement seen in the establishment of acquired immune receptors and their activation can be maintained by constant stimulation.

Also, as has been indicated, the bladder cancer cell line T24 expresses markedly down-modulated MHC class I molecules on its surface and the expression did not recover by the treatment with live BCG or live BCG-infected DCs. Thus, the T24 tumor would be recognized in a MHC molecule-unrestricted manner. Hence, we co-cultured the T24 cells with allogeneic PBMCs in the presence of live BCG and found a profound inhibition of tumor growth in vitro. A similar strong inhibition of T24 cell proliferation was observed when live BCG-infected DCs were co-cultured with PBMCs of the same donor. Moreover, the elimination of T24 cells was achieved mostly by CD3-positive innate effectors such as Vγ2Vδ2 TCR-expressing $\gamma\delta$T cells and NKT cells having predominant cytotoxicity, but not by class I MHC molecule-restricted conventional CD8β-positive CTLs, and the innate effectors were activated by live BCG-infected DCs rather than heat-inactivated BCG-treated DCs. Furthermore, the number of NKT cells but not $\gamma\delta$T cells or NK cells certainly increased in the live BCG-activated population.

These results strongly suggest that cells that control T24 tumor growth are not conventional class I MHC molecule-restricted $CD8^+$ CTL in the acquired arm but rather MHC molecule-unrestricted $\gamma\delta$T and NKT cells in the innate arm through the activation of DCs by live BCG. The results are reasonable in that continuous stimulation in the limited confined mucosal compartment of the bladder by a live organism may activate local innate effectors. Although the possible involvement of acquired effectors like $CD8^+$ CTLs in the prevention of surface bladder tumor expansion by intravesical BCG therapy has not be excluded, the data obtained in the present study strongly indicate a dominant effect of innate cells on tumor recurrence at the confined mucosal surface. Moreover, the cytotoxic effect of innate NKT or $\gamma\delta$T cells on T24 tumor cells was mediated thought stress-associated tumor-specific MICA/MICB molecules via their NKG2D receptors but not CD1d molecule-restricted invariant NKT-TCRs, indicating that these invariant TCRs are required mainly for their activation.

If this is the actual reason why intravesical BCG therapy is most successful immunotherapy against solid tumors in terms of preventing recurrence, we must focus on the constant activation of innate immunity for the treatment of other solid tumors and preventing their spread by metastasis. The findings shown in the present study will open the new notion that constant stimulation of innate effectors such as MHC molecule-unrestricted $\gamma\delta$T and NKT cells with live microorganisms like BCG through the activation of local DCs may provide a novel therapeutic way for cancer treatment.

Acknowledgments This work was supported in part by grants from the Ministry of Education, Science, Sport, and Culture, from the Ministry of Health and Labor and Welfare, Japan, and from the Japanese Health Sciences Foundation, and by the Promotion and Mutual Aid Corporation for Private School of Japan.